Production and detection of intermediate vector bosons and heavy leptons in pp and $\bar{p}p$ collisions

C. Quigg*

Fermi National Accelerator Laboratory,† P. O. Box 500, Batavia, Illinois 60510

Prospect for the discovery of the charged and neutral intermediate vector bosons in high-energy nucleon–(anti)nucleon collisions are examined. Theoretical arguments for the existence of intermediate bosons are reviewed and the anticipated properties are enumerated. Detailed calculations based on the Drell–Yan model are presented for the production cross sections and for the distributions of decay products. On the basis of these computations the requirement r experimental detectors are assessed.

CONTENTS

Foreword 297
I. Motivation for the Search 297
II. Properties of Intermediate Bosons and Heavy Leptons 298
A. The charged intermediate boson $W^{\pm}$ 298
B. The neutral intermediate boson Z^0 299
C. Heavy leptons 299
1. New sequential heavy lepton L with its own lepton number 300
2. Gauge theory heavy lepton with electron or muon number 301
D. Constraints from existing experiments 301
III. The Drell–Yan Model for Dilepton Production 301
IV. Production and Detection of $W^{\pm}$ 304
V. Production and Detection of Z^0 311
VI. Outlook 313
Acknowledgments 314
Appendix: Conserved Vector Current Relations for $W^{\pm}$ Production 314
References 315

FOREWORD

Observation of the intermediate vector boson, the mediator of weak interactions, has been a goal of elementary particle physics for many years. Why, then, is it necessary or desirable to examine again at this juncture the possibilities for producing and detecting the intermediate boson? On the experimental side, several artful and audacious designs of colliding beam facilities capable of attaining c.m. energies of several hundred GeV have been advanced. Theoretically, there is growing confidence that the intermediate boson mass is less than 100 GeV/c^2. These two considerations give the search for the intermediate boson a greater reality and perhaps even immediacy.

If we are to take best advantage of our opportunities, it is necessary to raise and try to answer a number of questions before experiments begin:

What are we searching for?
How copiously will it be produced?
How can it be detected?
What are the relative merits of pp and $\bar{p}p$ collisions?
What are the relative merits of various decay modes?

In the following pages I have addressed these issues, unburdened by the ardor that almost necessarily accompanies a proposal for an experiment or a facility. Since it appears very likely that machines of the next generation will make possible the discovery of the intermediate boson, detailed considerations which bear on experimental detection deserve our careful attention. I have also tried to identify areas in which further work is needed. In broad terms, these bear on the assumptions which underlie cross-section estimates and on experimental backgrounds and signatures.

He who estimates intermediate boson cross sections treads a well-traveled path. While I have certain pretensions to completeness and to a systematic approach, I am under no delusions of originality. My intent has been to produce, using orthodox techniques, a timely and useful reference manual with some cultural value. The fact that earlier calculations are mentioned only in passing should not be taken to mean that they have not influenced my outlook. The discovery of $J/\psi(3095)$, accumulating evidence for hadronic color, and improved knowledge of parton distributions have rendered obsolete the explicit results of many calculations. The prospect of very-high-energy $\bar{p}p$ collisions is relatively new. Furthermore, for my purpose of pulling together many aspects of the intermediate boson problem, it is simply efficient to do all the calculations from scratch. A large body of work which has been performed under the impulse of the ISABELLE Summer Studies at Brookhaven National Laboratory can be traced from the publications of Palmer *et al.* (1976) and Peierls *et al.* (1977).

I. MOTIVATION FOR THE SEARCH

The phenomenology of low-energy weak interactions is reproduced quite adequately by the familiar four-fermion point-coupling effective Lagrangian. The point-coupling description conflicts with unitarity at high energies, however. For example, the reaction

$$\nu_\mu e \to \mu \nu_e \tag{1.1}$$

proceeds entirely by s-wave scattering. Partial-wave unitarity requires

$$\sigma < \pi/2p^2 , \tag{1.2}$$

where p is the c.m. momentum of the colliding leptons, whereas in lowest order the point-coupling theory leads to

$$\sigma \approx 4G^2p^2/\pi , \tag{1.3}$$

where G is the Fermi coupling constant. The unitarity constraint is satisfied only for

$$p^4 < \pi^2/8G^2 , \tag{1.4}$$

*Alfred P. Sloan Foundation Fellow; also at Enrico Fermi Institute, University of Chicago, Chicago, Illinois 60637.

†Operated by Universities Research Association, Inc., under contract with the Energy Research and Development Administration.

i.e., for $p \lesssim 300$ GeV/c. The divergence of the point-coupling theory grows more severe in each order of perturbation theory. Therefore, as is well known, major revision is required to obtain a satisfactory theory.

A natural first step is to attempt to arrange a constant cross section at high energies by assuming, in analogy with quantum electrodynamics, that the weak interaction is mediated by exchange of a spin-one boson. Historically,[1] three properties have been imputed to the intermediate boson W:

1. It carries charge ± 1, because the familiar manifestations of the weak interaction (such as β decay) are charge-changing.
2. It must be rather massive, to reproduce the short-range of the weak force.
3. Its parity is indefinite.

Furthermore, its couplings to leptons and hadrons are fixed by the low-energy phenomenology. With the introduction of the $W^{\pm}$ of mass M_W, the cross section for $\nu_\mu e \to \mu \nu_e$ becomes

$$\sigma = 4G^2 p^2/\pi(1 + 4p^2/M_W^2) , \tag{1.5}$$

which approaches a constant value $G^2 M_W^2/\pi$ at high energies.

The result (1.5) is a great improvement over the point-coupling theory, but a problem persists: the s-wave scattering amplitude $\mathfrak{M}_0$ continues to violate partial-wave unitarity. A straightforward computation yields

$$\mathfrak{M}_0 = \frac{GM_W^2}{\pi\sqrt{2}} \log(1 + 4p^2/M_W^2) , \tag{1.6}$$

but partial-wave unitarity requires $\mathfrak{M}_0 < 1$, restricting the c.m. momentum to

$$p < \frac{M_W}{2}\left(\exp\left[\frac{\pi\sqrt{2}}{GM_W^2} \right] - 1 \right)^{1/2} . \tag{1.7}$$

This very mild unitarity violation occurs at incredibly high energies. It is not conquered in higher orders of perturbation theory because the $k_\mu k_\nu / M_W^2$ term in the W propagator makes the theory nonrenormalizable and gives rise to problems in higher order.

Gauge theories of the weak and electromagnetic interactions offer solutions to the problems of unitarity and renormalizability.[2] In view of the observation of neutral current phenomena, the introduction of a neutral intermediate boson Z^0 is attractive. Lacking a detailed phenomenology of neutral current interactions, we must appeal to specific models for the Z^0 couplings. Throughout this work I adopt the Weinberg–Salam model as a guide.

Heavy leptons bearing electron or muon number may also occur naturally in gauge theories and sequential heavy leptons bearing entirely new lepton numbers may well exist. Indeed there is some experimental evidence for the latter in the work of Perl and collaborators at SPEAR.[3] Furthermore, in gauge theories of the kind that now seems attractive, the existence of additional new quark flavors (beyond charm) implies the existence of additional leptons.[4] As a consequence, although our expectations for heavy leptons are perhaps more diffuse than for the intermediate bosons, we should be alert for indications of their presence.

There are, of course, many other hypothetical particles which have not been observed.[5] For the purposes of this document we shall, however, concentrate on intermediate bosons and heavy leptons. Let us now consider in more detail the characteristics these particles are expected to possess.

II. PROPERTIES OF INTERMEDIATE BOSONS AND HEAVY LEPTONS

A. The charged intermediate boson $W^{\pm}$

The leptonic decay modes

$$\begin{aligned} &W^+ \to \mu^+ \nu_\mu , \\ &W^+ \to e^+ \nu_e \end{aligned} \tag{2.1}$$

which are described by Fig. 1 are entirely fixed by the low-energy phenomenology. The partial width into any such mode is

$$\begin{aligned} \Gamma(W \to l\nu) &= GM_W^3/6\pi\sqrt{2} \\ &\simeq 4.4 \times 10^{-4}\ \text{MeV}\,[M_W/1\ \text{GeV}/c^2]^3 , \end{aligned} \tag{2.2}$$

and the normalized angular distribution of the decay lepton (l^- or ν) is

$$\frac{dN}{d\Omega} = \left\{ \begin{array}{ll} \frac{3}{16\pi}(1-\cos\theta)^2 & \lambda_W = 1 \\ \frac{3}{8\pi}\sin^2\theta & \lambda_W = 0 \\ \frac{3}{16\pi}(1+\cos\theta)^2 & \lambda_W = -1 \end{array} \right\} , \tag{2.3}$$

where λ_W is the helicity of the W.

The rate for the inclusive decay

$$W^{\pm} \to \text{hadrons} \tag{2.4}$$

can be computed in the framework of the quark model in analogy with the cross section for the reaction

$$e^+e^- \to \gamma_V \to \text{hadrons}. \tag{2.5}$$

The virtual photon decay into hadrons is represented in Fig. 2. For each quark flavor, one has

$$\Gamma(\gamma_V \to q_i \bar{q}_i) = \Gamma(\gamma_V \to \mu^+\mu^-) \times e_i^2 \times 3 , \tag{2.6}$$

where e_i is the quark charge, and the factor of three is a consequence of quark color. Consequently the ratio of hadronic to muonic cross sections is given by

$$R = \frac{\sigma(e^+e^- \to \text{hadrons})}{\sigma(e^+e^- \to \mu^+\mu^-)} = 3\sum_i e_i^2 , \tag{2.7}$$

which takes on the values $R = 2$ for three quarks (u, d, s),

[1] See, for example, Lee and Wu (1965).

[2] Gauge theories are explained lucidly by Abers and Lee (1973), and by Taylor (1976), among others.

[3] For experimental results, see Perl *et al.* (1975, 1976). Additional perspective on the search for heavy leptons may be gained from Perl and Rapidis (1974), and from Perl (1975).

[4] In models which are not "vectorlike," the cancellation of VVA anomalies requires that the charges of fermions sum to zero.

[5] A rather comprehensive list is given by Goldhaber and Smith (1975). Prospects for the identification of the Higgs boson of gauge theories are reviewed by Ellis, Gaillard, and Nanopoulos (1976).

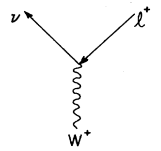

FIG. 1. Leptonic decay of the W^+.

and $R = \frac{10}{3}$ for four quarks (u, d, s, c). The SU(3) quark model prediction of $R = 2$ agrees reasonably with experimental data below the threshold for new physics (Augustin *et al.*, 1975). Without the factor of 3 for color, there would be utter disagreement. The representation of the inclusive hadronic decay in terms of $\gamma_V \to q\bar{q}$ suggests that individual hadronic events should display a jet structure, which has been observed (Hanson *et al.*, 1975).

In similar fashion we may compute the rates for the inclusive hadronic decay modes characterized as

$$W^+ \to u\bar{d} \ , \qquad W^+ \to u\bar{s} \ , \tag{2.8}$$

etc., as indicated in Fig. 3. The partial widths are

$$\Gamma(W^+ \to u\bar{d}) = \Gamma(W \to l\nu) \times \cos^2\theta_C \times 3 \ , \qquad \Gamma(W^+ \to u\bar{s}) = \Gamma(W \to l\nu) \times \sin^2\theta_C \times 3 \ , \tag{2.9}$$

where θ_C is the Cabibbo angle, and the factor of 3 is for color. More generally, if D_q is the number of weak doublets of quarks into which W can decay, the rate for the decay of $W \to$hadrons is given by

$$\Gamma(W \to \text{hadrons}) = \Gamma(W \to l\nu) \times 3 \times D_q \ . \tag{2.10}$$

Similarly, the total width is given by

$$\Gamma(W \to \text{all}) = \Gamma(W \to l\nu) \times (D_l + 3D_q) \ , \tag{2.11}$$

where D_l is the number of (accessible) weak doublets of leptons. Thus for Cabibbo theory, with two lepton doublets $\binom{\nu_e}{e}_L$ and $\binom{\nu_\mu}{\mu}_L$ and one quark doublet $\binom{u}{d_\theta}_L$, the muonic branching ratio is

$$\frac{\Gamma(W \to \mu\nu)}{\Gamma(W \to \text{all})} = \frac{1}{5} \ , \tag{2.12}$$

while for the minimal charm scheme, which incorporates an additional quark doublet $\binom{c}{s_\theta}_L$, it is

$$\frac{\Gamma(W \to \mu\nu)}{\Gamma(W \to \text{all})} = \frac{1}{8} \ . \tag{2.13}$$

The hadronic decays are expected to occur as back-to-back jets in the W rest frame. The normalized angular distribution of the decay quark, the direction of which defines a jet axis, is given by (2.3).

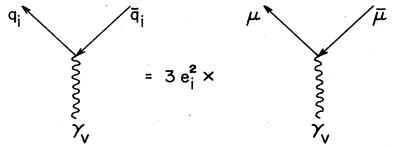

FIG. 2. Quark–parton model relation between inclusive hadronic and exclusive leptonic decays of a massive photon. Each quark is thought to fragment into a jet of hadrons.

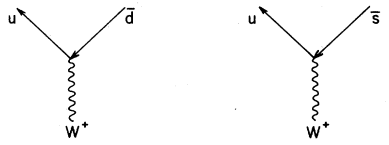

FIG. 3. Inclusive hadronic decays of the W^+.

B. The neutral intermediate boson Z^0

To anticipate the properties of the $W^\pm$ boson it was possible to rely on low-energy phenomenology and universality. Present knowledge of the neutral weak current is in contrast quite sketchy. Accordingly, it is necessary to adopt a specific model for the decays of the Z^0. The Weinberg–Salam model with four quarks (Weinberg, 1967, 1971; Salam, 1968, Glashow, Iliopoulos, and Maiani, 1970) provides a useful standard of reference.[6] In this model the neutral current couplings and the intermediate boson masses are specified by a single parameter known popularly as the Weinberg angle θ_W. (It will often be convenient to write $x_W = \sin^2\theta_W$.) The masses are given by

$$M_W^2 = M_Z^2(1 - x_W) = \pi\alpha / G x_W \sqrt{2} \ = (37.3 \text{ GeV}/c^2)^2 / x_W \ . \tag{2.14}$$

The leptonic decay widths are given by

$$\Gamma(Z^0 \to \nu\bar{\nu}) = G M_Z^3 / 12\pi\sqrt{2} \simeq 2.2 \times 10^{-4} \text{ MeV}[M_Z/1 \text{ GeV}/c^2]^3 , \tag{2.15}$$

and

$$\Gamma(Z^0 \to l^+ l^-) = \Gamma(Z^0 \to \nu\bar{\nu}) \times (1 - 4x_W + 8x_W^2). \tag{2.16}$$

Intermediate boson masses and leptonic partial widths according to the Weinberg–Salam model are plotted as functions of x_W in Fig. 4.

The inclusive rate for hadronic decays can be computed along the lines followed for W decay. The result is

$$\Gamma(Z^0 \to \text{hadrons}) = \Gamma(Z^0 \to \nu\bar{\nu}) \times (2 - 4x_W + 40x_W^2/9) \times 3 \times D_q , \tag{2.17}$$

where 3 is a color factor, and $D_q = 2$. The branching fractions derived from Eqs. (2.15)–(2.17) are plotted in Fig. 5. It is noteworthy that for values of the Weinberg angle favored[7] by current experiments $(0.3 \lesssim x_W \lesssim 0.4)$ the branching ratio for e^+e^- or $\mu^+\mu^-$ decay is approximately 5%.

C. Heavy leptons

It is possible to make some very simple estimates of charged heavy-lepton branching ratios in the "asymptotic" mass regime where masses of the products are

[6] A convenient guide to the phenomenology is given by De Rujula, Georgi, Glashow, and Quinn (1974).

[7] See, for example, Albright, Quigg, Shrock, and Smith (1976), and Lee (1976).

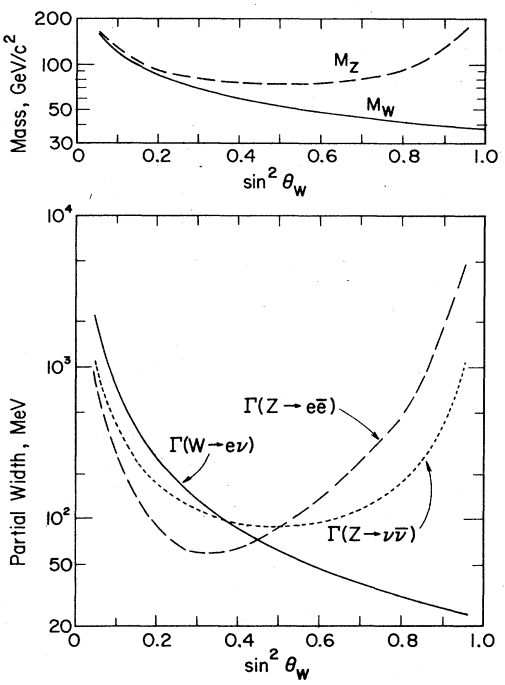

FIG. 4. Masses and leptonic partial widths of $W^{\pm}$ and Z^0 in the Weinberg–Salam model, as functions of the Weinberg angle. The regime $0.3 < \sin^2\theta_W < 0.4$ is favored by neutrino scattering experiments.

unimportant and semileptonic decays are treated inclusively. There are two important cases:

1. New sequential heavy lepton L with its own lepton number

The rate for leptonic decay, computed from Fig. 6, is given by

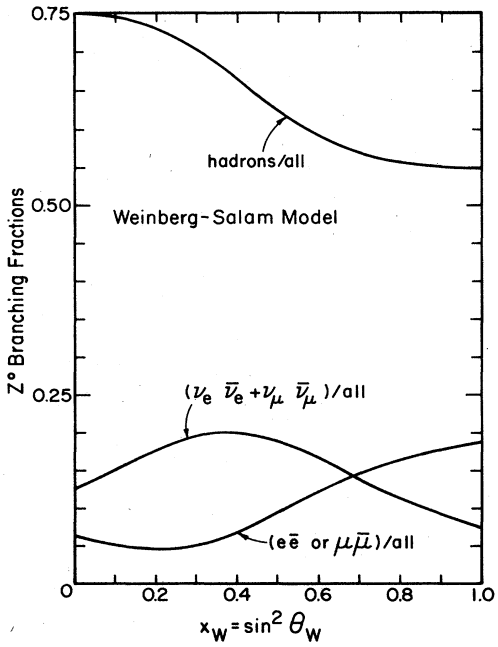

FIG. 5. Z^0 branching fractions in the four colored quark Weinberg–Salam model, as functions of the Weinberg angle.

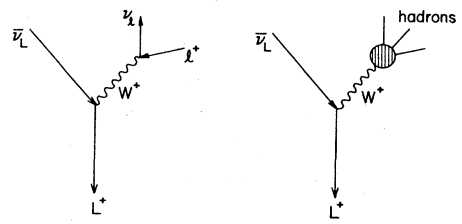

FIG. 6. Leptonic and semileptonic decays of a heavy lepton L^+.

$$1/\tau_0 \equiv \Gamma(L^+ \to l^+ \nu_l \bar{\nu}_L) = G^2 M_L^5/192\pi^3 \tag{2.18}$$

in the limit of large W mass, an expression familiar from muon decay. The resulting partial lifetime, τ_0, is shown in Fig. 7 as a function of the heavy-lepton mass. For this case the branching ratios of the charged heavy lepton are precisely those of the virtual W. Thus

$$\frac{\Gamma(L \to \text{all})}{\Gamma(L \to e\nu_e \nu_L)} = D_l + 3D_q\,, \tag{2.19}$$

where the number of lepton and quark doublets counted are those for which the decays are energetically allowed.

For a heavy lepton of about 2 GeV/c^2 mass[8] we would expect, in the minimal model,

$$\frac{\Gamma(L \to e\nu_e \nu_L)}{\Gamma(L \to \text{all})} = \frac{\Gamma(L \to \mu\nu_\mu \nu_L)}{\Gamma(L \to \text{all})} = 20\%, \qquad \frac{\Gamma(L \to \text{hadrons} + \nu_L)}{\Gamma(L \to \text{all})} = 60\%\,. \tag{2.20}$$

A more massive heavy lepton L' which could decay into charmed hadrons plus the 2 GeV/c^2 heavy lepton would give

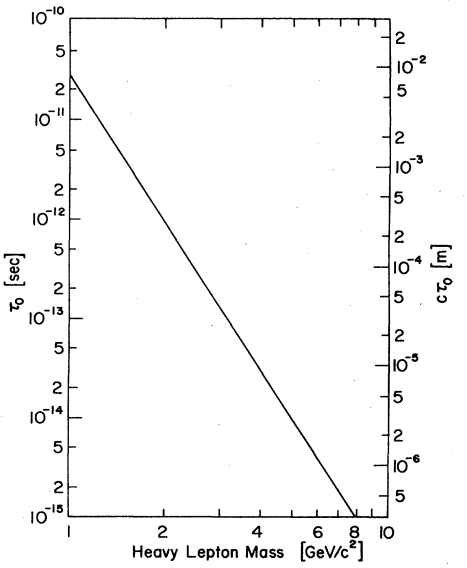

FIG. 7. "Partial lifetime" τ_0, defined in Eq. (2.18), for heavy-lepton decay, as a function of lepton mass.

[8] As suggested by the μe events observed at SPEAR; see the references in Footnote 3.

$$\frac{\Gamma(L'\to e\nu_e\nu_{L'})}{\Gamma(L'\to\text{all})}=\frac{\Gamma(L'\to\mu\nu_\mu\nu_{L'})}{\Gamma(L'\to\text{all})}=\frac{\Gamma(L'\to L\nu_L\nu_{L'})}{\Gamma(L'\to\text{all})}=\frac{1}{9}\,,$$
$$\frac{\Gamma(L'\to\text{hadrons}+\nu_{L'})}{\Gamma(L'\to\text{all})}=\frac{2}{3} \qquad (2.21)$$

and so forth.

2. Gauge theory heavy lepton with electron or muon number

This case, for which charge equals lepton number, has been examined in detail (Bjorken and Llewellyn-Smith, 1973; Tsai, 1971). Consider a massive E^+ carrying electronic lepton number. By an analysis equivalent to the foregoing, we find

$$\Gamma(E\to\mu\nu_\mu\nu_e)=\tfrac{1}{2}\Gamma(E\to e\nu_e\nu_e)=G^2M_E^5/192\pi^3. \qquad (2.22)$$

Again the remaining branching ratios are those of the virtual W. For a 2 GeV/c^2 E^+, the branching ratios are

$$\frac{\Gamma(E\to\mu\nu_\mu\nu_e)}{\Gamma(E\to\text{all})}=\frac{1}{6}\,,$$
$$\frac{\Gamma(E\to e\nu_e\nu_e)}{\Gamma(E\to\text{all})}=\frac{1}{3}\,, \qquad (2.23)$$
$$\frac{\Gamma(E\to\text{hadrons}+\nu_e)}{\Gamma(E\to\text{all})}=\frac{1}{2}\,,$$

in agreement with Fig. 5 of Bjorken and Llewellyn-Smith (1973). For a massive gauge muon, the electronic and muonic modes are interchanged.

D. Constraints from existing experiments

Experimental results allow us to place some approximate lower bounds on the intermediate boson masses. From the absence of propagator effects in the νN total cross section the Caltech–Fermilab Collaboration Sciulli, 1975) deduces $M_W>14$ GeV/c^2 (90% confidence limit). Measurements of the quantity $\langle\nu\rangle=\langle Q^2/s\rangle$ in deep-inelastic νN scattering by the Harvard–Pennsylvania–Wisconsin–Fermilab Collaboration (Cline, 1975) imply $M_W>27$ GeV/c^2 (90% C.L.). The absence of signals for $W^\pm$ production in νN, μN, and γN collisions at Fermilab can also be translated into (more model-dependent) limits. Since the W apparently has not been pair-produced in experiments at SPEAR, we may infer $M_W>3.8$ GeV/c^2. Similarly, nonobservation of the Z^0 in Bhabha scattering at SPEAR implies $M_{Z^0}>7.6$ GeV/c^2.

Recently Bjorken (1976) has estimated bounds on the intermediate boson masses, assuming the weak and electromagnetic interactions to be based upon a spontaneously broken gauge theory with an underlying simple gauge group. Typically M_W lies between 55 and 75 GeV/c^2, but the bounds on M_{Z^0} are much less restrictive.

III. THE DRELL-YAN MODEL FOR DILEPTON PRODUCTION

The starting point for our investigation of intermediate boson production will be the model developed by Drell and Yan (1970, 1971) to describe the production of massive lepton pairs in hadron–hadron collisions.[9] Although this procedure carries with it considerable model dependence, I prefer it to the "model-independent" application of conserved vector current (CVC) arguments [reviewed in the Appendix] to data on massive lepton pair production (Okun, 1966; Yamaguchi, 1966; Lederman and Pope, 1971). In large part my preference is due to the paucity of data on massive dilepton production over a wide range of energies. Indeed, at this time the CVC arguments would be useless for $\bar{p}p$ collisions.

In the quark–parton model,[10] the cross section for the hadronic reaction

$$a+b\to c+\text{anything} \qquad (3.1)$$

is given by

$$\sigma(a+b\to c+\text{anything})=\sum_{\{q\}}P_a(q_1)P_b(q_2)\sigma(q_1+q_2\to c+\text{anything})\,, \qquad (3.2)$$

where $P_i(q_j)$ is the probability of finding quark q_j in hadron i, and $\sigma(q_1+q_2\to c+\text{anything})$ is the cross section for the elementary process leading to the desired final state. The summation runs over all contributing quark configurations. Drell and Yan (1970, 1971) treated the reaction illustrated in Fig. 8,

$$a+b\to l^+l^-+\text{anything} \qquad (3.3)$$

in which a lepton pair of invariant mass $\mathfrak{M}$ is produced with c.m. momentum fraction x in collisions at c.m. energy $s^{1/2}$. The differential cross section is given by

$$\frac{d\sigma}{d\mathfrak{M}^2dx}=\left(\frac{4\pi\alpha^2}{3\mathfrak{M}^4}\right)F(\tau,x)\,, \qquad (3.4)$$

where the function

$$F(\tau,x)=\frac{x_ax_b}{(x^2+4\tau)^{1/2}}\,g(x_a,x_b) \qquad (3.5)$$

depends upon the scaled variable

$$\tau=\mathfrak{M}^2/s\,. \qquad (3.6)$$

Information about the quark distributions within the hadrons is contained in the function

$$g(x_a,x_b)=\frac{1}{3}\sum_{\substack{\text{flavors}\\ i}}e_i^2[q_a^{(i)}(x_a)\bar{q}_b^{(i)}(x_b)+\bar{q}_a^{(i)}(x_a)q_b^{(i)}(x_b)]\,, \qquad (3.7)$$

where e_i is the charge of quark flavor i, $q_a^{(i)}(x_a)$ is the probability of finding quark i with momentum fraction x_a in hadron a, and $\bar{q}$ refers to antiquarks. The factor

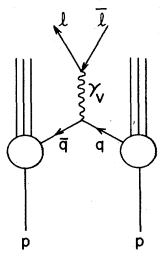

FIG. 8. The Drell-Yan mechanism for massive lepton-pair production in pp collisions.

[9] A recent critical review is provided by Sullivan (1976).

[10] Many applications of this philosophy are described by Berman, Bjorken, and Kogut (1971).

$\frac{1}{3}$ is a consequence of color: the quark and antiquark that annihilate into a virtual photon must have the same color as well as flavor. The kinematical variables x_a and x_b of the elementary process are related to those of the hadronic process by

$$x_{a,b} = \tfrac{1}{2}[(x^2 + 4\tau)^{1/2} \pm x]\,. \tag{3.8}$$

The integrated cross section for dilepton production is

$$\frac{d\sigma}{d\mathfrak{M}^2} = \frac{4\pi\alpha^2}{3\mathfrak{M}^4}\,\tau \int_\tau^1 \frac{dx\, g(x, \tau/x)}{x}\,. \tag{3.9}$$

The Drell–Yan picture carries a number of significant implications. The most general of these is the *scaling prediction* that $\mathfrak{M}^4 d\sigma/d\mathfrak{M}^2$ should be a function of τ alone. Second, if the quark (parton) distributions $q_a^{(i)}(x_a)$ are known, specific predictions can be made on the basis of (3.4) or (3.9) for dilepton cross sections. In the case of nucleons, data on deep-inelastic lepton scattering provide substantial information on the parton distributions, and many parametrizations have appeared in the literature. I have compared several of these (Blankenbecler *et al.*, 1975; Minh Duong-Van, 1976; Altarelli *et al.*, 1975; Pakvasa, Parashar, and Tuan, 1974; Farrar, 1974; Finjord and Ravndal, 1976; Field and Feynman, 1976) with the leptoproduction data (Perkins, 1975; Taylor, 1975; Mo, 1975) and with the elementary sum rules (Feynman, 1972). On the basis of this comparison I have selected two distributions which are in respectable agreement with electron and neutrino scattering experiments and which represent, in my view, reasonable extremes of parton parametrizations. Of the two, the Pakvasa–Parashar–Tuan (PPT) parametrization contains a broad $x^{-1}(1-x)^{7/2}$ sea quark distribution, whereas the Field parametrization incorporates a more conservative $x^{-1}(1-x)^7$ sea quark distribution.[11] I have a mild, and purely subjective, preference for the latter.

At the present time there are insufficient data outside the region of known resonances (which are apparently not produced by the Drell–Yan process) to test Drell–Yan *scaling*. Recent measurements (Hom *et al.*, 1976a, b; Kluberg *et al.*, 1976) of dilepton production in p-nucleus collisions at 400 GeV/c by the Columbia–Fermilab–Stony Brook and Chicago–Princeton Collaborations do permit a test of the Drell–Yan prediction. These are compared in Fig. 9 with predictions based upon the PPT and Field parton distributions. Roughly speaking, the data lie within the swath bounded by the two theoretical curves, a necessary but not sufficient condition for accepting the Drell–Yan formula. Even assuming that the agreement is not coincidental, the data do not select one parton distribution over the other, as they are confined to the small-τ region in which the two predictions differ by no more than one order of magnitude. The accumulation of data at other energies and at higher values of τ is of prime importance.

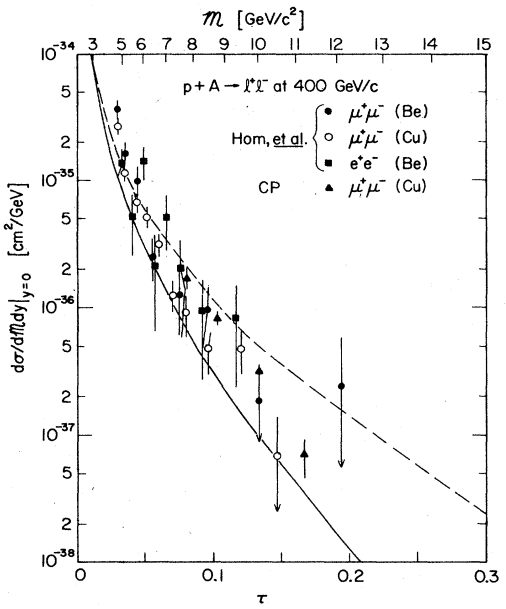

FIG. 9. Comparison of the Drell–Yan model with data on dilepton production at c.m. rapidity $y = 0$ by 400 GeV/c protons on nuclear targets. The cross sections per nucleon are displayed, assuming linear A dependence. Computations were performed for beryllium; the neutron to proton ratio of copper is nearly identical. The solid curve is calculated using Field's parton distributions. The dashed curve is for the PPT parametrization. Data are from Hom *et al.* (1976a,b), and Kluberg *et al.* (1976). The abscissa is $\tau = \mathfrak{M}^2/s$.

The scaled longitudinal momentum distribution $s\,d\sigma/d\tau\,dx$ is shown in Fig. 10 for several choices of τ, for pp collisions. Although the gross features are dictated by kinematics, the differences between the two sets of predictions are sensitive to details of the parton distributions. The scaling function for the integrated cross section is shown as a function of $\sqrt{\tau}$ in Fig. 11 for the reactions $p^\pm p \to l^+l^- + \text{anything}$. Because of the presence of valence antiquarks in the antiproton, the cross section for dilepton production is expected to be larger in $\bar{p}p$ collisions than in pp collisions. The difference can be quite large: it approaches three orders of magnitude for $\sqrt{\tau} = \frac{1}{2}$ in the Field parametrization. There is as yet no test of this prediction. It has, however, been shown (Anderson *et al.*, 1976) that high-mass pairs are more effectively produced in πN than in pN collisions. For small values of $\sqrt{\tau}$, the presence or absence of valence antiquarks is of much less consequence.

The Drell-Yan model carries a further implication of experimental interest. Consider the production of lepton pairs in $\pi^\pm$ collisions on an isoscalar target such as carbon. Since the Drell–Yan process is intrinsically electromagnetic, it implies (Mockett *et al.*, 1975) a specific violation of isospin invariance. Define the ratio

$$\rho = \frac{d\sigma}{d\mathfrak{M}^2}(\pi^+ C \to l^+l^- + X) \Big/ \frac{d\sigma}{d\mathfrak{M}^2}(\pi^- C \to l^+l^- + X)\,. \tag{3.10}$$

If the pairs are produced through noninterfering reso-

[11] Aficionados of parton distributions will be aware of a recent paper by Okada, Pakvasa, and Tuan (1976), claiming that their $x^{-1}(1-x)^{7/2}$ sea distribution is unique in surviving experimental tests. They refer to experiments on massive dilepton production and to the poorly known $x \to 0$ behavior of νW_2 in deep-inelastic electron scattering. The former are entirely compatible with an $x^{-1}(1-x)^7$ parametrization (see Fig. 9 below) and the latter is insensitive to the parametrization chosen for $x \to 1$. Their arguments are thus incorrect; the Field parametrization is an explicit counterexample.

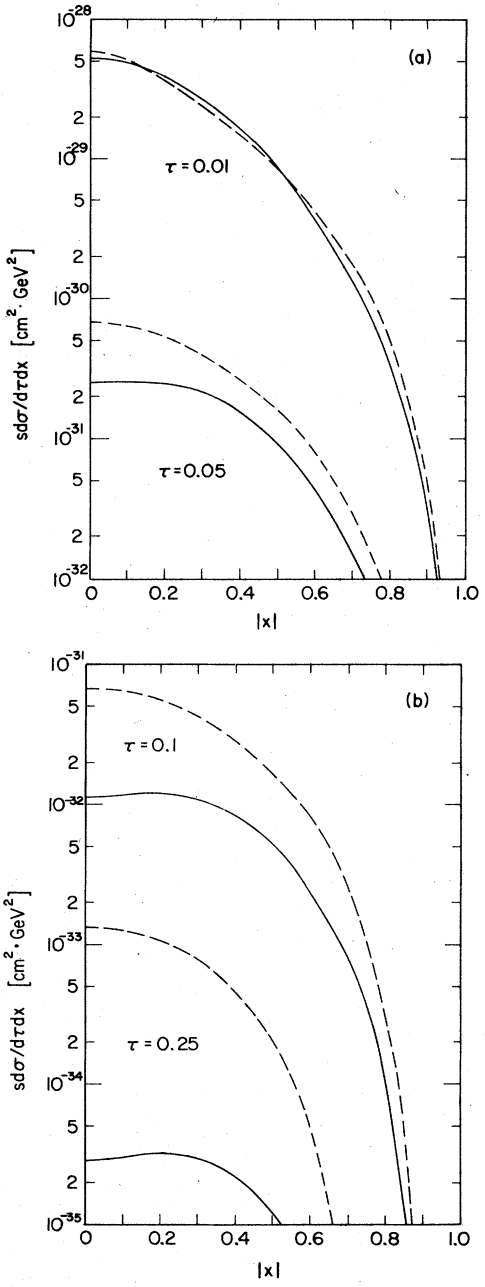

FIG. 10. Scaled longitudinal momentum distribution for Drell–Yan production of dileptons in pp collisions. The solid (dashed) curves correspond to the Field (PPT) parton distribution.

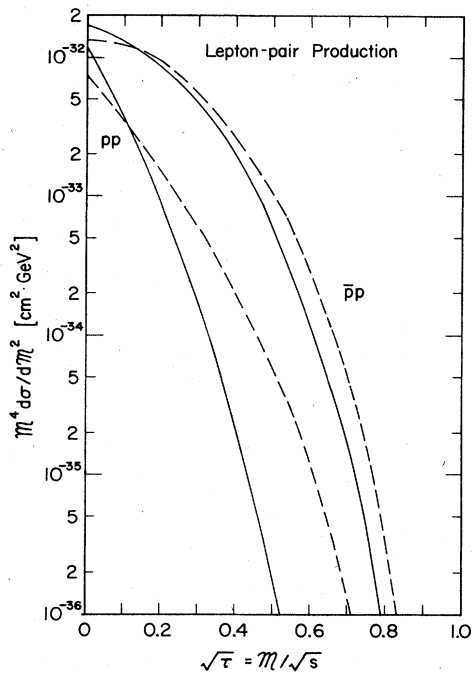

FIG. 11. Scaling function for the integrated cross sections for dilepton production in pp and $\bar{p}p$ collisions. The solid (dashed) curves correspond to the Field (PPT) parton distribution.

nances in

$$\pi^{\pm} C \to \text{hadron} + X \quad \text{(with } \hookrightarrow l^+l^-\text{)}, \tag{3.11}$$

$\rho = 1$, but if they are produced through

$$\pi^{\pm} C \to \gamma_V + X \quad \text{(with } \hookrightarrow l^+l^-\text{)}, \tag{3.12}$$

$\rho \neq 1$ in general. An extreme example of the latter is Drell–Yan production by valence quark annihilation. For incident π^+, the elementary process is $d\bar{d} \to \gamma_V$; for incident π^- it is $u\bar{u} \to \gamma_V$. The cross section is proportional to the square of the quark charge, so we find

$$\rho = \tfrac{1}{4}. \tag{3.13}$$

In a less schematic Drell–Yan model, with valence and sea quarks, the value $\rho = \frac{1}{4}$ is attained only for rather large lepton pair masses. At very small masses, for which sea quarks–sea quark annihilations are dominant, $\rho \to 1$. The ratio ρ has now been measured, and exhibits the trend anticipated by the Drell–Yan model (Anderson *et al.*, 1976).

It is usual to assume, as an idealization, that partons carry no transverse momentum. As a consequence, the dileptons produced by the Drell–Yan mechanism must carry no (i.e., small) transverse momentum. Those observed with high masses at 400 GeV/c have $\langle p_\perp \rangle \simeq 1$ GeV/c (Hom *et al.*, 1976a, b; Kluberg *et al.*, 1976; Cronin, 1976). The experimental results raise two issues: First, does $\langle p_\perp \rangle$ remain sufficiently small at large masses that it can be accommodated in the Drell–Yan picture by relaxing the idealization that quarks carry no transverse momentum? Second, how severely will the detection of intermediate bosons be compromised if the W is produced with appreciable $\langle p_\perp \rangle$? I shall adopt the point of view that a nonzero but small $p_\perp$ is an inconsequential annoyance which can be neglected at the level of credibility merited by the following calculations. It is well to keep in mind, however, that things could be worse than they appear.

In summary, the Drell–Yan model is in comfortable agreement with existing data on high-mass lepton pairs, but it is far from established. The scaling prediction

has yet to be tested[12] and the finite $\langle p_\perp \rangle$ of the pairs is not neatly understood. Additional experiments in proton, antiproton, and pion beams are of immense practical importance.

Before leaving the subject of massive lepton pairs it is appropriate to comment on the production of massive pairs of heavy leptons. The cross-section computations of this section carry over to heavy leptons without essential change, so cross sections are not paltry for $\tau \lesssim \frac{1}{4}$. Experimental detection is likely to be quite challenging, however.[13] As indicated in Fig. 7, the heavy leptons will decay before reaching a detector. Their presence will be signaled by μe coincidences, as in

$$p + p \to L^+ + L^- + \text{anything}, \quad L^+ \to e^+ \bar{\nu}_e \nu_L, \quad L^- \to \mu^- \nu_\mu \bar{\nu}_L \tag{3.14}$$

a tantalizing but hardly definitive signature. It appears that study of heavy leptons will fall principally to e^+e^- machines.

IV. PRODUCTION AND DETECTION OF $W^\pm$

The cross section for the reaction

$$a + b \to W^\pm + \text{anything} \tag{4.1}$$

in which an intermediate boson of mass M_W is produced with c.m. momentum fraction x in collisions at c.m. energy $s^{1/2}$ can be computed in direct fashion in the Drell–Yan picture.[14] The elementary processes of importance are $u + \bar{d} \to W^+$, $u + \bar{s} \to W^+$, $\bar{u} + d \to W^-$, and $\bar{u} + s \to W^-$. The differential cross section is given by

$$d\sigma/dx = G\pi\sqrt{2}\, H(\tau, x), \tag{4.2}$$

where the function

$$H(\tau, x) = \frac{x_a x_b}{(x^2 + 4\tau)^{1/2}}\, W_{ab}^{(\pm)}(x_a, x_b) \tag{4.3}$$

depends upon the scaled variable

$$\tau = M_W^2/s. \tag{4.4}$$

The quark–quark interaction is described by the function

$$W_{ab}^{(+)}(x_a, x_b) = \tfrac{1}{3}\{[u_a(x_a)\bar{d}_b(x_b) + \bar{d}_a(x_a)u_b(x_b)]\cos^2\theta_C + [u_a(x_a)\bar{s}_b(x_b) + \bar{s}_a(x_a)u_b(x_b)]\sin^2\theta_C\}, \tag{4.5}$$

where the variables x_a and x_b are given by (3.8) and $u(x)$, $d(x)$, ... are quark distribution functions. Quarks and antiquarks are interchanged for W^- production. The integrated $W^\pm$ cross section is

$$\sigma_{W^\pm} = G\pi\sqrt{2}\,\tau \int_\tau^1 \frac{dx\, W_{ab}^{(\pm)}(x, \tau/x)}{x}. \tag{4.6}$$

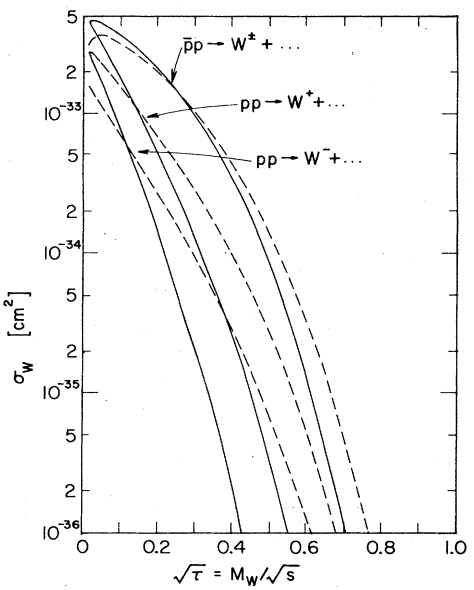

FIG. 12. Cross sections for $W^\pm$ production in pp and $\bar{p}p$ collisions in the Drell–Yan model. The dashed (solid) lines refer to the PPT (Field) parton distribution. Turnovers near $\sqrt{\tau} = 0$ are artifacts of the parton distributions near $x = 0$, which are inadequately known.

Integrated cross sections for $W^\pm$ production in pp and $\bar{p}p$ collisions are shown in Fig. 12 as functions of $\sqrt{\tau} = M_W/\sqrt{s}$. In pp collisions the production of W^- is suppressed relative to W^+ by a factor of two or more because of the smaller momentum fraction carried by down quarks compared with up quarks. The cross sections for W^+ and W^- production are necessarily equal in $\bar{p}p$ collisions. As in the case of dilepton production, the competitive advantage of antiproton beams is small at low values of $\sqrt{\tau}$ and becomes significant for $\sqrt{\tau} \gtrsim \frac{1}{2}$, especially for the Field parametrization. However, for values of $\sqrt{\tau}$ large enough that the ratio $\sigma_W(\bar{p}p)/\sigma_W(pp)$ exceeds 10^2 in the Field parametrization, the $\bar{p}p$ cross section is itself small, on the order of 10^{-35} cm^2.

The angular distribution of the produced W's and, more to the point, the angular distributions of the decay products are of great importance for the design of experiments. Expressed in terms of c.m. rapidity (pseudorapidity for the decay products), these distributions depend on the c.m. energy only through the scaled variable $\tau = M_W^2/s$. The computed angular distributions will be displayed for $\tau = 0.02$, 0.10, and 0.25, for pp and $\bar{p}p$ collisions, and for my two choices of quark distributions. However it will suffice to discuss only one case in detail.

The differential cross sections for W^+ and W^- production in pp collisions at $\tau = 0.1$, according to the Drell–Yan model with the PPT parton parametrization, are shown in Fig. 13. Both are substantially confined to the region $|y| < 1$. The important differential cross sections

[12] A recent test by Lederman and Pope (1976) offers some encouragement.

[13] In this context, see Bhattacharya, Smith, and Soni (1976), and Chu and Gunion (1975). The Drell–Yan cross section for heavy-lepton pairs is $(1 - 4M_L^2/\mathfrak{M}^2)^{1/2}(1 + 2M_L^2/\mathfrak{M}^2)$ times the electron pair cross section. The kinematical suppression is <10%, for $\mathfrak{M} \gtrsim 3M_L$.

[14] Many estimates of the cross sections for W production have appeared in the literature. A representative list includes Finjord (1976), Rubbia, McIntyre, and Cline (1976), Paschos and Wang (1976), Palmer, Paschos, Samios, and Wang (1976), Okun and Voloshin (1976), Halzen (1976), Golubkov, Ivanilov, Nikitin, and Rozhnov (1974).

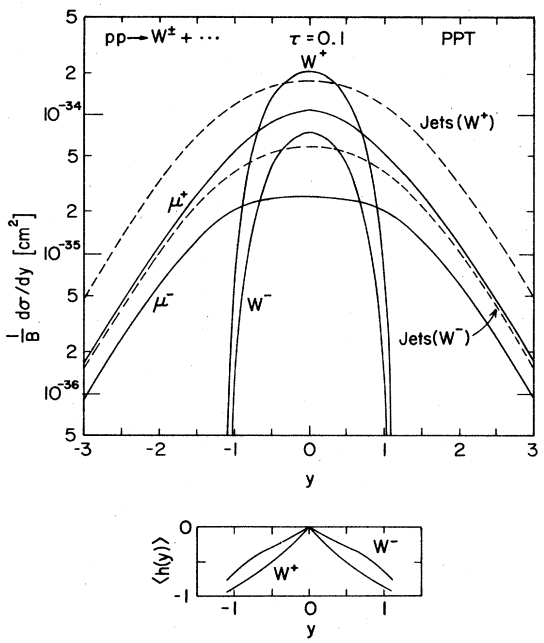

FIG. 13. Angular distributions for $pp \to W^{\pm} + \cdots$ at $\tau = 0.1$, in terms of c.m. rapidity y, and for the decay products $\mu^{\pm}$ and hadron jets. [For the decay products pseudorapidity is used.] Also shown is the net helicity of the produced $W^{\pm}$ as a function of rapidity. Based on the PPT parton parametrization. Curves for decay products have not been multiplied by branching ratios.

for the decay products may be computed from these results and the decay angular distributions (2.3), provided the production cross sections are known for definite W-helicity.

Since the $Wq\bar{q}$ coupling has a $V-A$ structure, the W is produced with helicity -1 if the c.m. momentum of the quark exceeds that of the antiquark and with opposite helicity if the momenta are interchanged. The mean helicity,

$$\langle h(y)\rangle \equiv \left[\frac{d\sigma}{dy}(\lambda_W = +1) - \frac{d\sigma}{dy}(\lambda_W = -1)\right] \Big/ \frac{d\sigma}{dy}\,, \qquad (4.7)$$

is displayed in Fig. 13. Away from $y = 0$ most of the cross section is generated by the scattering of energetic valence quarks, so $\langle h(y)\rangle \to -1$. At $y = 0$ the symmetry of the situation ensures that $\langle h(y)\rangle = 0$. The rate of the transition between these two extremes is determined by the momentum distribution of the sea quarks.

To appreciate the consequences of this polarization for the distributions of detected leptons, consider the extreme case of $\langle h(y)\rangle = -1$. The μ^+ from W^+ decay is emitted preferentially along the direction of spin of the W^+. It will therefore be thrown *toward* $y = 0$. In contrast, the μ^- from W^- decay is emitted preferentially along the direction opposite to the spin of the W^-. It will therefore be thrown *away from* $y = 0$. These effects are clearly apparent in Fig. 13, which shows the differential cross section for μ^+ concentrated near $y = 0$ and a relatively flatter distribution for μ^-.

Also shown in Fig. 13 are the differential cross sections for hadronic decays. What is plotted is the sum of

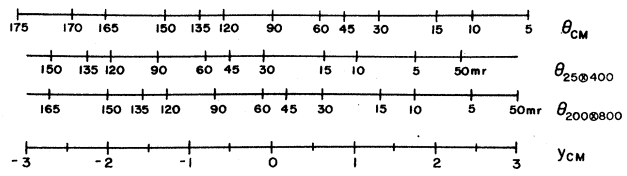

FIG. 14. Correspondence of angles to the c.m. rapidity scale used in other figures. The angle scales refer to collisions of equal energy beams, to 25⊗400 GeV/c collisions, and to 200 ⊗800 GeV/c collisions.

cross sections for the quark and antiquark from $W^{\pm}$ decay, for which the value of $\langle h(y)\rangle$ is irrelevant. Thus the shapes of the jet distributions for W^+ and W^- production and decay are nearly identical, reflecting only the small difference in the production angular distributions.

The angular extent of a detector which would be sensitive to a large fraction of W decays is considerable: the interval $45^\circ < \theta_{\text{c.m.}} < 135^\circ$ may be barely adequate. The translation from c.m. rapidity to laboratory angle is made in Fig. 14 for the lab = c.m. configuration and for two asymmetric beam momentum configurations.

The differential cross sections for W^+ and W^- production and decay in pp collisions at $\tau = 0.1$, computed using Field's parton distribution, are shown in Fig. 15. With this parametrization the C-violating character of the weak decay is shown even more clearly, as the μ^- distribution is peaked near $|y| = 1$.

The influence of W polarization is actually most profound in the case of $\bar{p}p$ collisions. The production angular distribution of W^- according to the PPT parametrization is shown in Fig. 16 for $\tau = 0.1$. The maximum in the differential cross section occurs in the forward ($\bar{p}$) hemisphere, near $y = 0.2$, where negative particle production is favored by the projectile charge. For W^+ production, the situation is precisely reversed. Intermediate bosons produced in $\bar{p}p$ collisions will be more intensely polarized than those produced in pp collisions. In the backward hemisphere, the quark nearly always is more energetic than the antiquark. The opposite is true in the forward hemisphere. Consequently, the *spin* of the produced W is strongly aligned along the antipro-

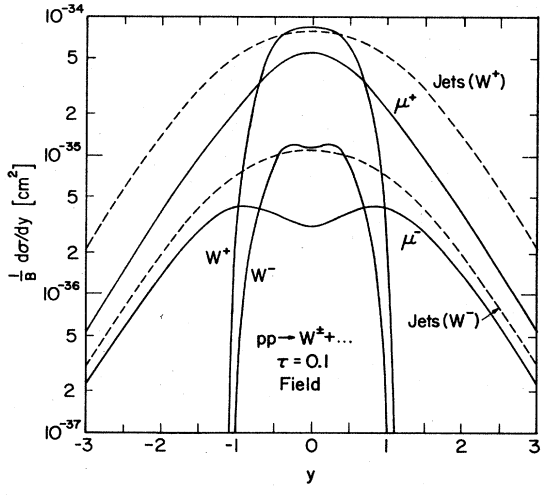

FIG. 15. Same as Fig. 13, for the Field parton distribution.

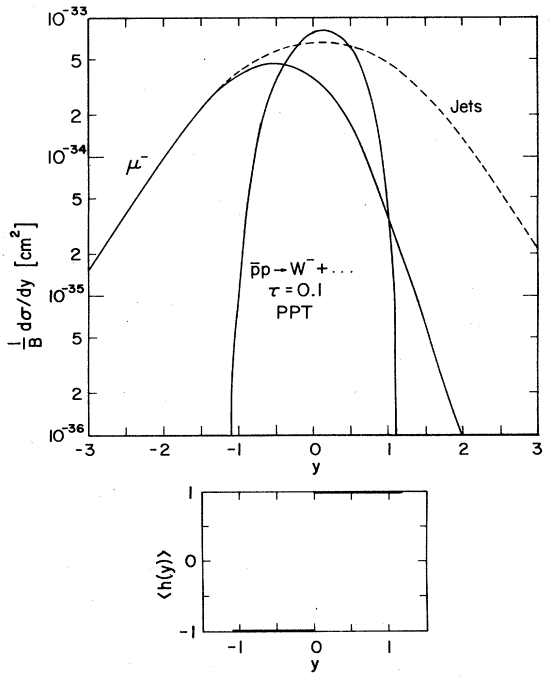

FIG. 16. Angular distribution for $\bar{p}p \to W^- + \cdots$ at $\tau = 0.1$. Curves apply to the production and decay of W^+ with the replacement $y \longleftrightarrow -y$. Also shown is the net helicity of the produced $W^\pm$ as a function of rapidity. Based on the PPT parametrization. Curves for decay products have not been multiplied by branching ratios.

ton direction. The helicity $\langle h(y) \rangle$ is near -1 for $y < 0$ and near $+1$ for $y > 0$, as shown in Fig. 16. This means that the decay μ^- from W^- decay is thrown *along the proton direction*. Indeed, the μ^- differential cross section is peaked near $y = -0.5$, in the *proton* hemisphere. This very counterintuitive prediction follows from the $V-A$ structure of the W coupling to fermions. Once again, the angular distribution of hadronic jets is not affected by the W alignment. It peaks in the forward hemisphere, whence it came. The corresponding cross sections, computed using the Field distribution, are plotted in Fig. 17.

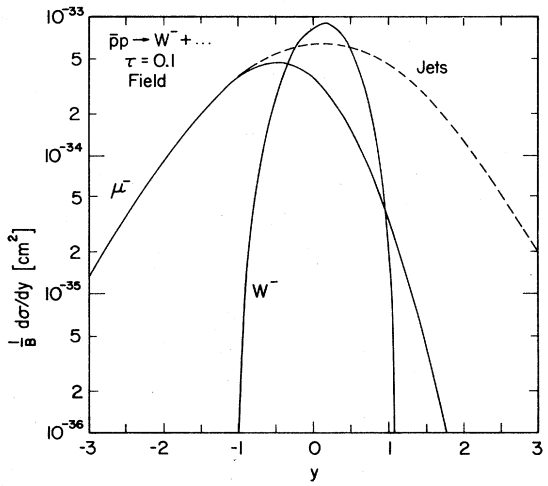

FIG. 17. Same as Fig. 16, for the Field parton distribution.

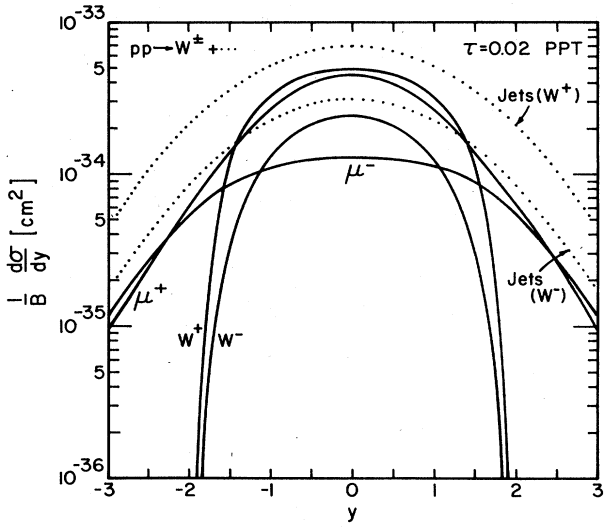

FIG. 18. Same as Fig. 13, for $\tau = 0.02$.

Similar comments apply to the calculations for $W^\pm$ production at $\tau = 0.02$ and 0.25 displayed in Figs. 18–25.

For the leptonic decays $W \to \mu\nu, e\nu$ the neutrino is undetectable, so the mass of the W must be inferred from the transverse momentum distribution of the charged decay product. It is therefore of interest to ask, in the context of the Drell–Yan model, what degree of mass discrimination is to be expected. In the idealization employed here, the intermediate vector boson is produced with zero transverse momentum. The conclusions are qualitatively unchanged if the W is given a small mean transverse momentum (a few GeV/c), but mass discrimination degenerates quickly as $\langle p_\perp \rangle$ approaches a significant fraction of M_W.

Again let us look in detail at the case of $\tau = 0.1$. The qualitative observations to be made do not depend upon the quark distribution, so I shall display results only for the PPT parametrization. The transverse momentum spectrum of μ^+ from the reaction $p + p \to W^+ +$ anything is shown in Fig. 26 in terms of the scaled variable

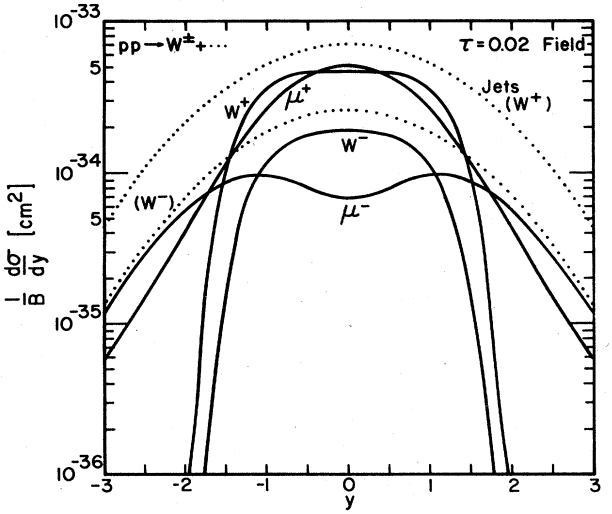

FIG. 19. Same as Fig. 18, for the Field parton distribution.

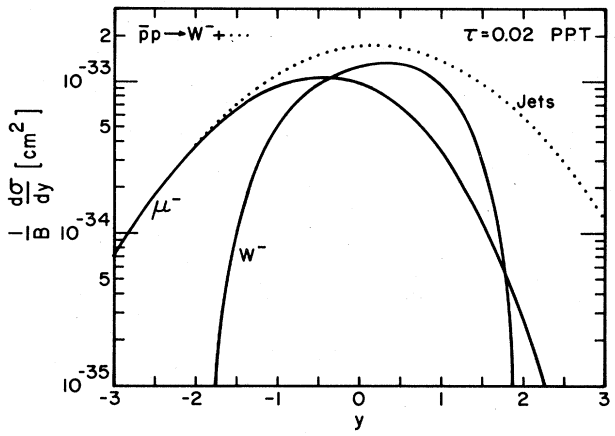

FIG. 20. Same as Fig. 16, for $\tau = 0.02$.

$$x_\perp \equiv 2p_\perp/M_W \tag{4.8}$$

for several values of c.m. rapidity. At $y = 0$ and $|y| = 0.5$ a pronounced Jacobian peak is apparent near $x_\perp = 1$. However, for $|y| = 1$, where the cross section $d\sigma_\mu/dy$ remains significant, the $p_\perp$ distribution displays only a tiny peak near $x_\perp = 1$. A general lesson is that not all of the cross section implied by Fig. 12 and the appropriate branching ratio will provide useful mass discrimination, even in the best of circumstances ($\langle p_\perp \rangle = 0$). The expectations for the decay $W^- \to l^- \nu$ are shown in Fig. 27. They are entirely analogous. Conditions for intermediate boson production in $\bar{p}p$ collisions are, if anything, slightly less favorable because of the expected strong alignment of the W. The curves in Fig. 28 show excellent discrimination (for W^- production) at $y = 0.5$, fair discrimination at $y = -0.5$, and none at all at $y = -1.5$, where $d\sigma_\mu/dy$ exceeds the value at $y = 0.5$. As for pp collisions, not all the production cross section is useful for mass measurement. The corresponding predictions for $\tau = 0.02$ and $\tau = 0.25$ are given in Figs. 29–34.

It has been suggested that the hadronic decays of the

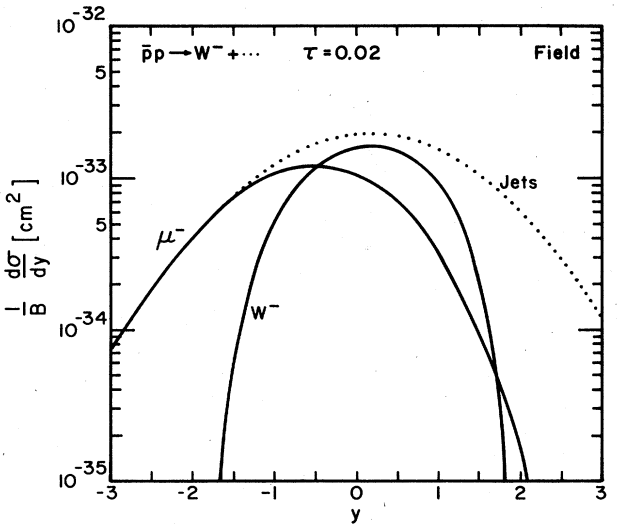

FIG. 21. Same as Fig. 20, for the Field parton distribution.

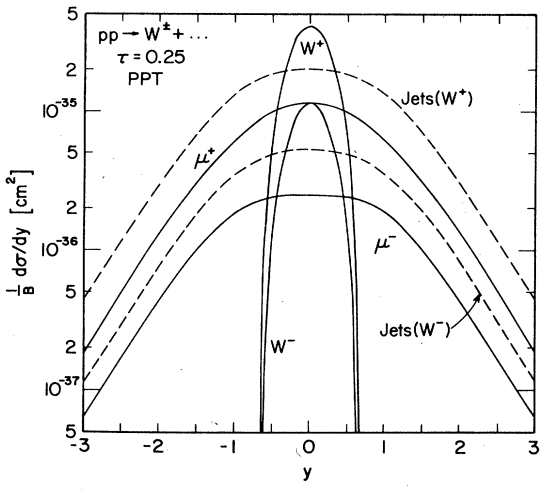

FIG. 22. Same as Fig. 13, for $\tau = 0.25$.

W are potentially more informative than the leptonic decays because the invariant mass of the W can be reconstructed. To achieve good mass resolution will require excellent hadron calorimetry for charged and neutral particles. The limiting factor is likely to be the ambiguity problem posed by low transverse momentum hadrons: Are they to be included in the hadron jets, or are they extraneous? A rough guess,[15] guided by current knowledge of large transverse momentum phenomena, is that ± 10% mass resolution is the best that can be expected, assuming perfect calorimetry.

Let us put aside these practicalities for the time being and study the problems of jet detection in the idealized setting of the quark–parton model. For the hadronic decays, the Jacobian peak in the transverse momentum distribution can be put to two uses. First, as for the leptonic decays, measurement of the total transverse momentum of a jet provides a measure of the intermediate boson mass. The second asset of the Jacobian peak for hadronic decays is to provide a preselection of jets for the effective mass reconstruction. A single ex-

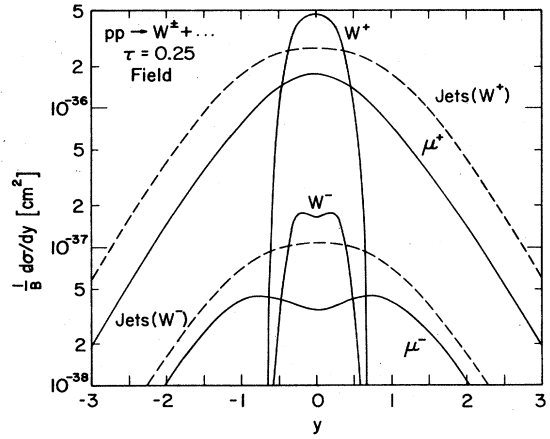

FIG. 23. Same as Fig. 22, for the Field parton distribution.

[15] I thank S. Brodsky and R. D. Field for advice on this point.

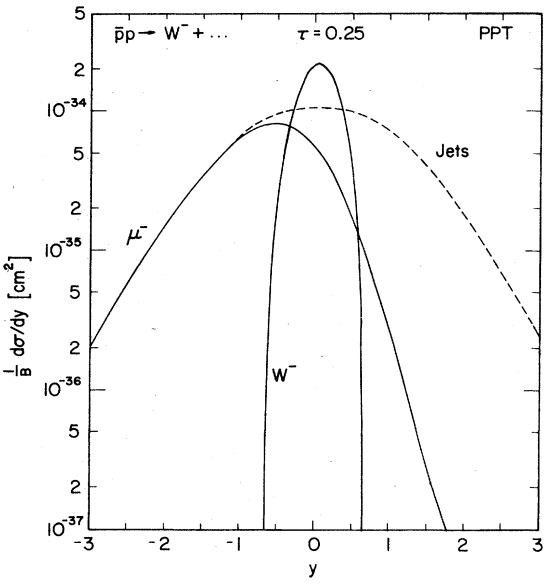

FIG. 24. Same as Fig. 16, for $\tau = 0.25$.

ample of the transverse momentum spectrum of jets is given in Fig. 35, which shows that the prominence of the Jacobian peak for jets is quite comparable to that for leptons.

Correlations expected among jets may also influence the design of a detector. The predicted correlations are shown in Figs. 36–39 for $\tau = 0.1$ and $\tau = 0.25$. The principal qualitative feature is that in general the second jet will lie in the hemisphere opposite the first, because the differential cross section for W production is confined to small values of $|y|$. These correlations give additional impulse to the requirement for a large-aperture detector.

The background to hadronic jets from W decay is an issue which deserves considerable study. I shall present merely an introduction to the problem which indicates the need for further thought. To do so, I focus on

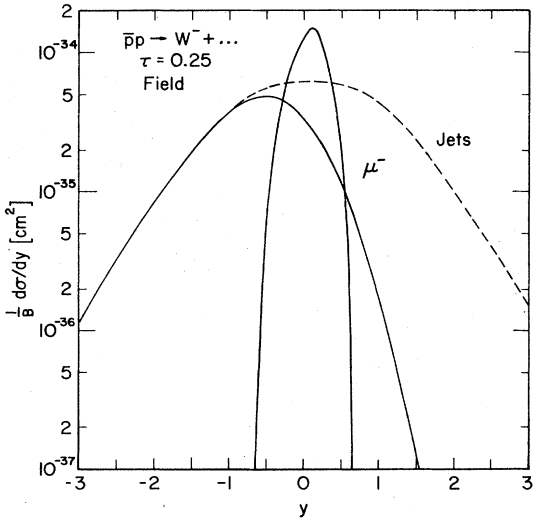

FIG. 25. Same as Fig. 24, for the Field parton distribution.

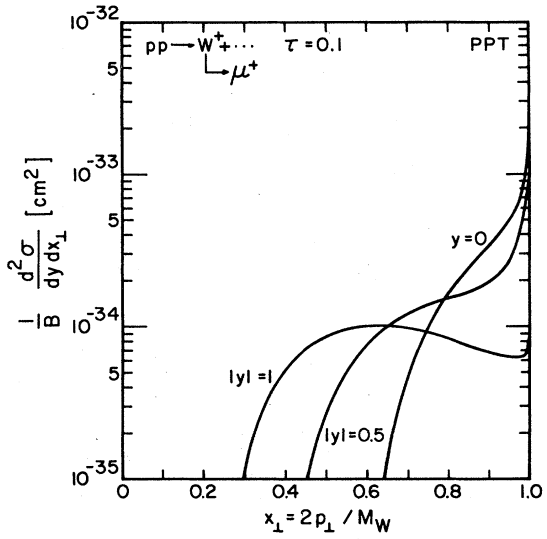

FIG. 26. Transverse momentum distribution of μ^+ from W^+ decay for $\tau = 0.1$ in pp collisions, showing the $(1 - x_\perp^2)^{-1/2}$ Jacobian peak for small values of $|y|$. The finite width of the W has been neglected. Curves refer to the PPT parton distribution; those for the Field parametrization are similar in character.

the integral transverse momentum spectrum to be expected in pp collisions at $y = 0$, adopting the Weinberg–Salam model with $x_W = 0.3$ to fix the mass of the intermediate boson. Predictions for $\sqrt{s} = 224$ GeV, corresponding to $\tau = 0.1$, are displayed in Fig. 40. The dotted curve shows the integral spectrum from the production and hadronic decay of W^+ and W^-, assuming a 75% hadronic branching ratio. The sharp step in the integral spectrum at $p_\perp = M_W/2$ reflects the prominent Jacobian peak in the differential spectrum. On this scale the width of the W (~ 1.2 GeV) can be neglected.

Two sorts of background (at least) may be anticipated. The first is the "ordinary" hadronic background due to large transverse momentum collisions. This may be

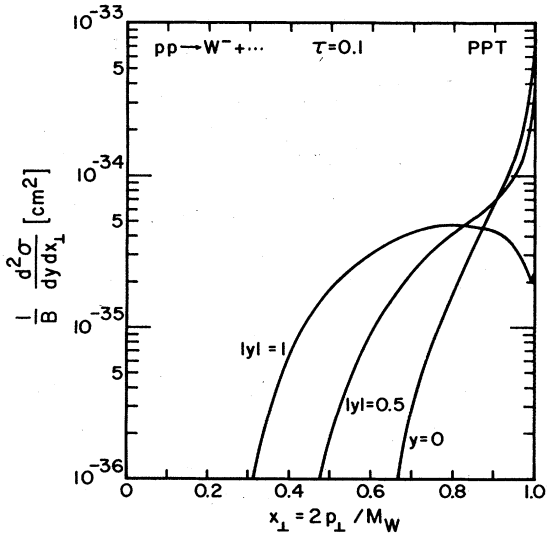

FIG. 27. Same as Fig. 26, for $pp \to W^-$ production and leptonic decay.

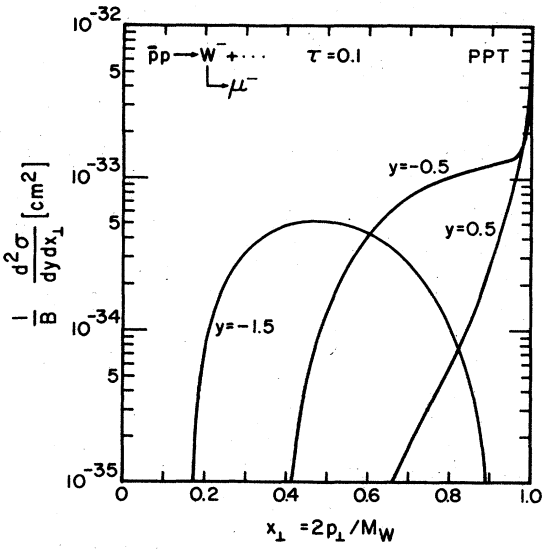

FIG. 28. Same as Fig. 26, for $\bar{p}p \to W^-$ production and leptonic decay. The curves apply to W^+ with the replacement $y \to -y$.

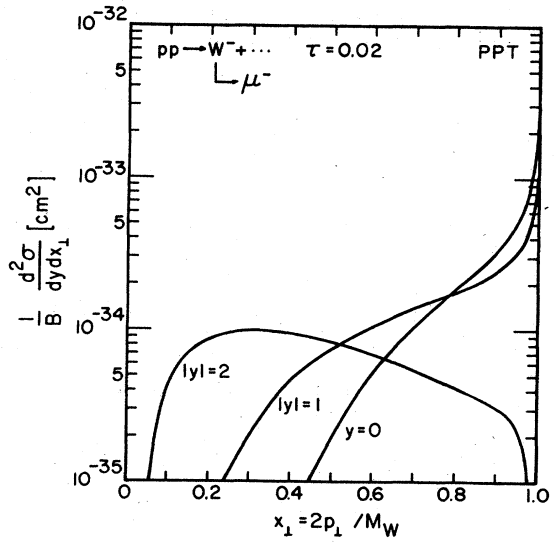

FIG. 30. Same as Fig. 27, for $\tau = 0.02$.

estimated using one of the now popular hard scattering models, in which

$$d\sigma_{\text{jet}}/(d^3p/E) = p_\perp^{-n} f(p_\perp/\sqrt{s}). \tag{4.9}$$

Existing data are well described[16] by a form proportional to $p_\perp^{-8}$. To be somewhat conservative, I have adopted the parametrization proposed by Field and Feynman (1976), which is on the high side of current models. The extraction of a jet cross section from measured single-hadron cross sections is highly model dependent. The quark–quark scattering mechanism of Field and Feynman requires a larger jet cross section to achieve a given single hadron cross section than does the constituent interchange model.[17] The high-$p_\perp$ background predicted by the Field–Feynman parametrization is indicated by the long-dashed line in Fig. 40. The sum of the background estimate and the cross section due to W decay is plotted as a thin solid curve. Although the step in the integral distribution is rather clear, it is evident that if the background were an order of magnitude larger, the signal would be obscured.

A second, potentially quite annoying, source of background is the decay of the neutral intermediate boson Z^0 into hadrons. The cross-section computation is discussed in some detail in Sec. V. The resulting integral distribution is plotted as the short-dashed curve in Fig. 40. Because of the proximity of W and Z masses in the Weinberg–Salam model, it presents a significant source of confusion for the jets from W decay. The total integral spectrum, the thick solid curve in Fig. 40, is a challenging target for experiments. The same remarks apply to pp collisions at a higher energy, $\sqrt{s} = 500$ GeV, as shown in Fig. 41.

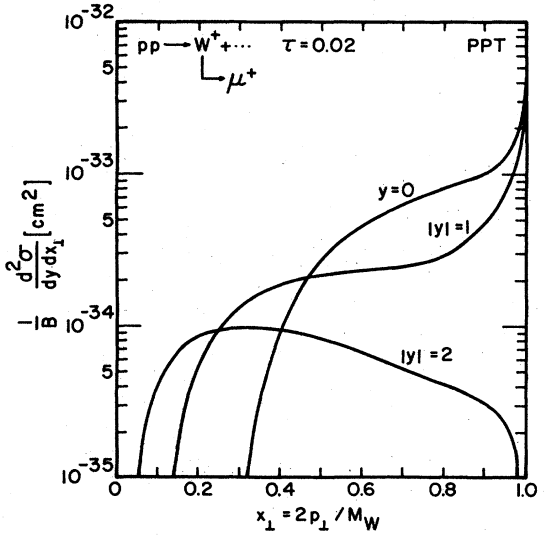

FIG. 29. Same as Fig. 26, for $\tau = 0.02$.

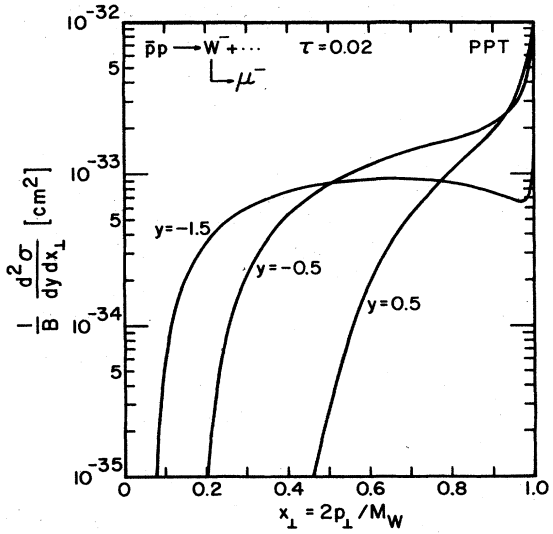

FIG. 31. Same as Fig. 28, for $\tau = 0.02$.

[16] For recent reviews of experiment and theory, see Darriulat (1976), Fox (1976), and Frisch (1976).

[17] For a review, see Sivers, Brodsky, and Blankenbecler (1976).

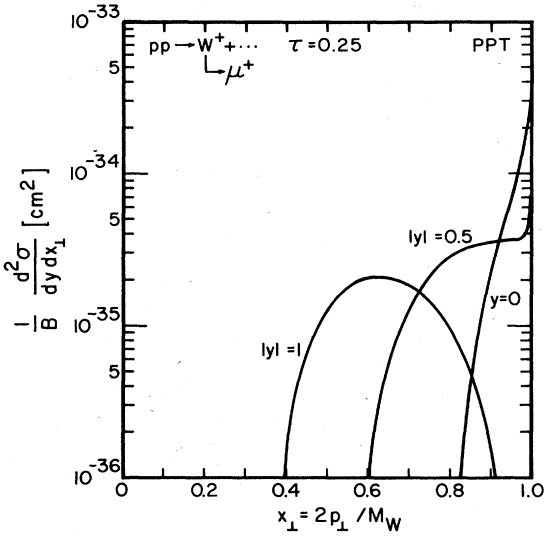

FIG. 32. Same as Fig. 26, for $\tau = 0.25$.

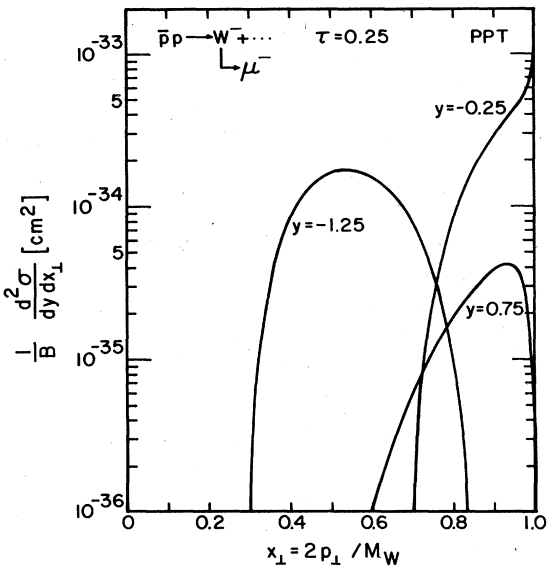

FIG. 34. Same as Fig. 28, for $\tau = 0.25$.

There are two further background questions which should be addressed before leaving the subject of W production. One concerns the relative importance of background in $\bar{p}p$ collisions as compared with pp collisions. Unfortunately there is no experimental information which can be used as a guide. We must therefore resort to theology. In hard scattering models which have been used to describe large $-p_\perp$ phenomena, the ordinary hadronic background is expected to increase less than the signal from W and Z^0 decay when the projectile is changed from proton to antiproton. (See Footnote 15, above.) If this is so, $\bar{p}p$ collisions would have a better signal-to-background ratio than pp collisions by a factor of up to 5 at $\sqrt{s} = 224$ GeV and up to 3 at $\sqrt{s} = 500$ GeV. Measurements of large transverse momentum phenomena in $\bar{p}p$ collisions at the energies of present accelerators would be most illuminating. The second important question deals with the single-hadron background for the leptonic decay. This is expected (Field and Feynman, 1976) to be one or two orders of magnitude smaller than the hadronic jet background shown in Figs. 40 and 41, whereas the W-decay signal would drop by a factor of approximately 6 (assuming the Weinberg–Salam model branching ratios). Furthermore, a high-$p_\perp$ muon from W decay is accompanied by an undetected neutrino with opposite transverse momentum, whereas hadronic events will result in jets on both sides of the beam direction.

Some final words of caution are in order. If the Field parton distribution is used, there is a slightly smaller signal-to-expected-background ratio at the energies considered here, which may be judged from Fig. 12. The signal still appears detectable, if the $p_\perp^{-8}$ background estimate is representative. A $p_\perp^{-4}$ hadronic background, which may be envisaged on dimensional grounds (Berman, Bjorken, and Kogut, 1971), could well swamp

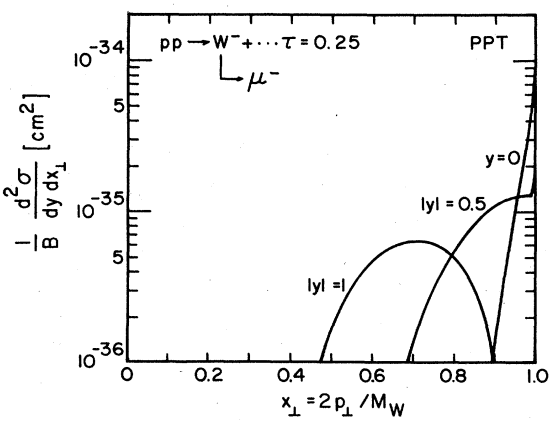

FIG. 33. Same as Fig. 27, for $\tau = 0.25$.

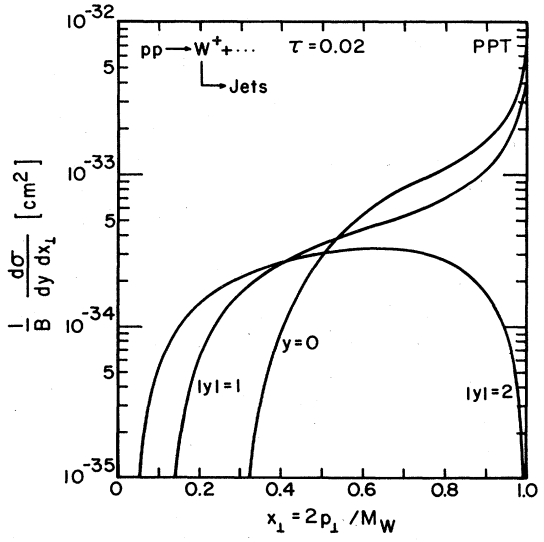

FIG. 35. Transverse momentum distribution of hadronic jets from W^+ decay for $\tau = 0.02$ in pp collisions. Curves refer to the PPT parton distribution.

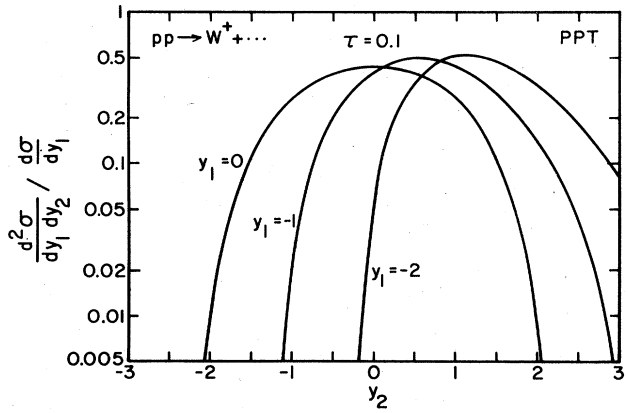

FIG. 36. Jet-jet correlations for production and hadronic decay of W^+ in pp collisions for $\tau=0.1$. Curves are based on the PPT parton distribution. Predictions for $pp\to W^-$ and those based on the Field parton distribution are essentially identical.

any hadronic signal.[18] The largest $p_\perp^{-4}$ component which could have gone undetected in the large-transverse-momentum experiments carried out to date[19] would give rise to backgrounds at $p_\perp = 30$ GeV/c approximately two orders of magnitude larger than those shown in Figs. 40 and 41.

V. PRODUCTION AND DETECTION OF Z^0

As I stressed in Sec. II, any discussion of the properties of the neutral intermediate vector boson Z^0 is necessarily quite model dependent because of the primitive state of our understanding of neutral current phenomena. Without further apology I will adopt the Weinberg–Salam model to fix the couplings of Z^0 to quarks and leptons.[20]

The cross section for the reaction

$$a + b \to Z^0 + \text{anything} \tag{5.1}$$

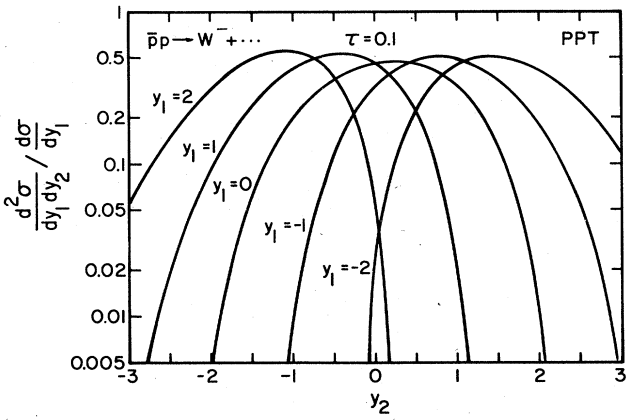

FIG. 37. Same as Fig. 36, for $\bar{p}p\to W^-+\cdots$. The curves apply to W^+ production and decay with the replacements $y_{1,2}\leftrightarrow -y_{1,2}$.

[18]In this vein, a maximum credible disaster analysis was undertaken by Halzen (1976). I regard his dire predictions as unreasonable, but not impossible.

[19]I am grateful to R. D. Field for providing a parametrization of this possibly hidden component.

[20]Jaffe and Primack (1973) have considered Z^0 production in other gauge models.

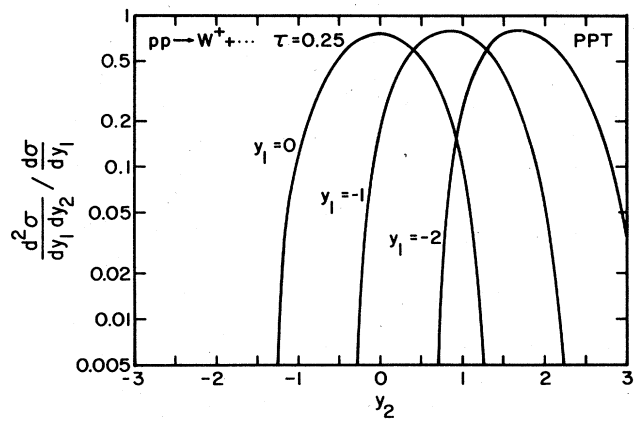

FIG. 38. Same as Fig. 36, for $\tau=0.25$.

in which an intermediate boson of mass M_Z is produced with c.m. momentum fraction x at c.m. energy $s^{1/2}$ can be computed using the Drell–Yan picture, in terms of the elementary processes $u\bar{u}\to Z^0$, $d\bar{d}\to Z^0$, $s\bar{s}\to Z^0$. The differential cross section can be written as

$$d\sigma/dx = 2G\pi\sqrt{2}K(\tau, x), \tag{5.2}$$

where the function

$$K(\tau, x) = \frac{x_a x_b}{(x^2+4\tau)^{1/2}} Z_{ab}(x_a, x_b) \tag{5.3}$$

depends upon the scaled variable

$$\tau = M_Z^2/s. \tag{5.4}$$

The elementary interactions are described by the function

$$\begin{aligned} Z_{ab}(x_a, x_b) = \frac{1}{3}\Big\{ &[u_a(x_a)\bar{u}_b(x_b) + \bar{u}_a(x_a)u_b(x_b)]\left[\frac{1}{4} - \frac{2x_W}{3} + \frac{8x_W^2}{9}\right] \\ &+ [d_a(x_a)\bar{d}_b(x_b) + \bar{d}_a(x_a)d_b(x_b) + s_a(x_a)\bar{s}_b(x_b) \\ &+ \bar{s}_a(x_a)s_b(x_b)]\left[\frac{1}{4} - \frac{x_W}{3} + \frac{2x_W^2}{9}\right]\Big\}, \end{aligned} \tag{5.5}$$

where $x_W = \sin^2\theta_W$, the variables x_a and x_b are given by (3.8), and $u(x)$, $d(x)$, ... are quark distribution functions. The integrated Z^0 cross section is

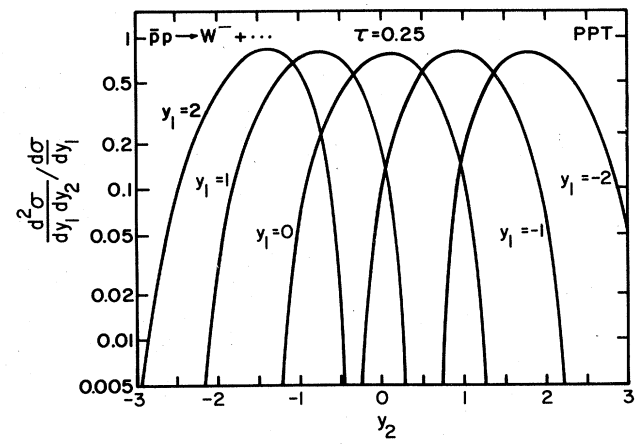

FIG. 39. Same as Fig. 37, for $\tau=0.25$.

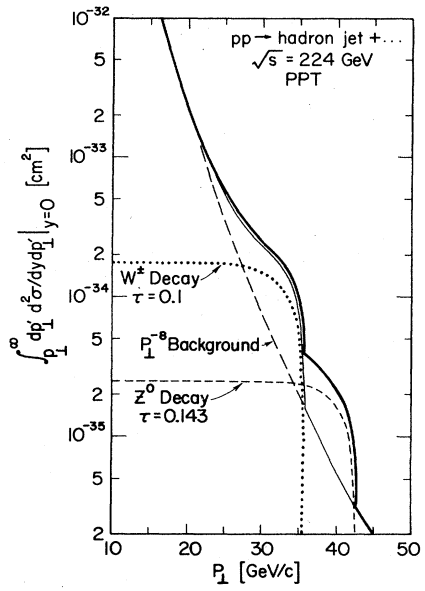

FIG. 40. Integral transverse momentum spectrum for hadron jets produced at $y=0$ in 224 GeV pp collisions. Weinberg–Salam model values for intermediate boson masses and branching ratios have been assumed. Cross sections for $W^{\pm}$ and Z^0 production refer to the PPT distribution. The curves are explained in the text.

$$\sigma_{Z^0} = 2G\pi\sqrt{2}\tau \int_{\tau}^{1} \frac{dx Z_{ab}(x, \tau/x)}{x} . \tag{5.6}$$

Integrated cross sections for Z^0 production in pp and $\bar{p}p$ collisions are shown in Fig. 42 as functions of $\sqrt{\tau} = M_Z/\sqrt{s}$, for $x_W = 0.3$.[21] As usual, the competitive advantage of $\bar{p}p$ collisions is significant only for $\sqrt{\tau} \gtrsim \frac{1}{2}$.

The differential cross sections for Z^0 production in pp collisions at $\tau = 0.1$ and 0.25, according to the Drell–Yan model with the PPT parton parametrization, are shown in Fig. 43. These are confined to small values of

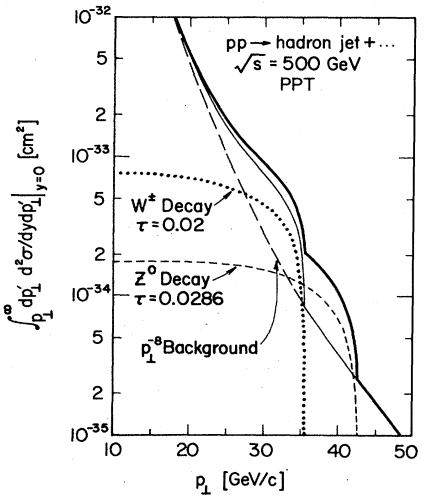

FIG. 41. Same as Fig. 40, for 500 GeV pp collisions.

[21]The sensitivity to x_W, within the range preferred by neutral current phenomenology, is not acute.

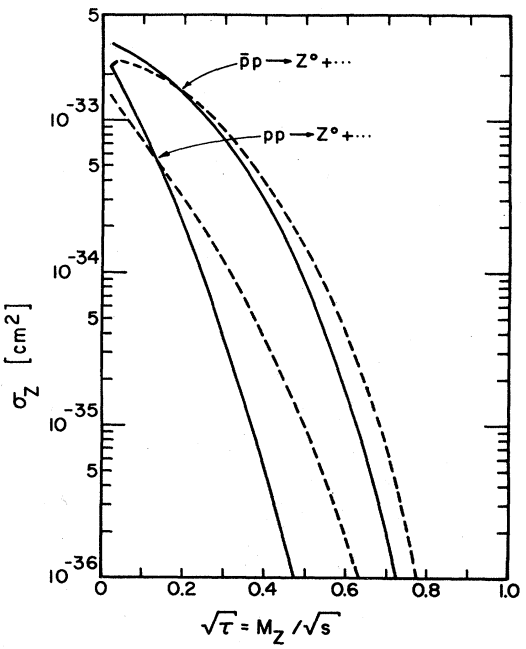

FIG. 42. Cross sections for Z^0 production in pp and $\bar{p}p$ collisions in the Drell–Yan model with $\sin^2\theta_W = 0.3$. The dashed (solid) lines refer to the PPT (Field) parton distribution. Turnovers near $\sqrt{\tau} = 0$ are artifacts of the parton distributions near $x = 0$, which are inadequately known.

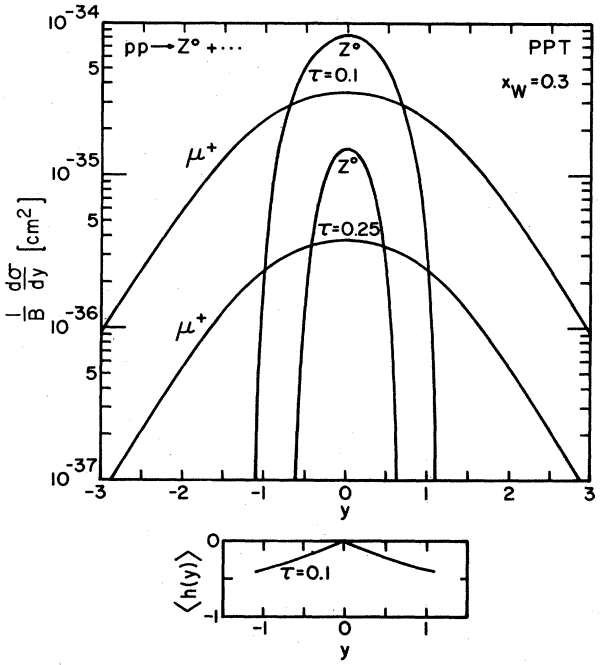

FIG. 43. Angular distributions for $pp \to Z^0 + \cdots$ at $\tau = 0.1$ and 0.25, in terms of c.m. rapidity y, and for the decay μ^+, for $\sin^2\theta_W = 0.3$. [For the decay products pseudorapidity is used.] For the decay μ^- the distribution is nearly identical. The PPT parton distribution is used. The net helicity of the produced Z^0 is shown as well.

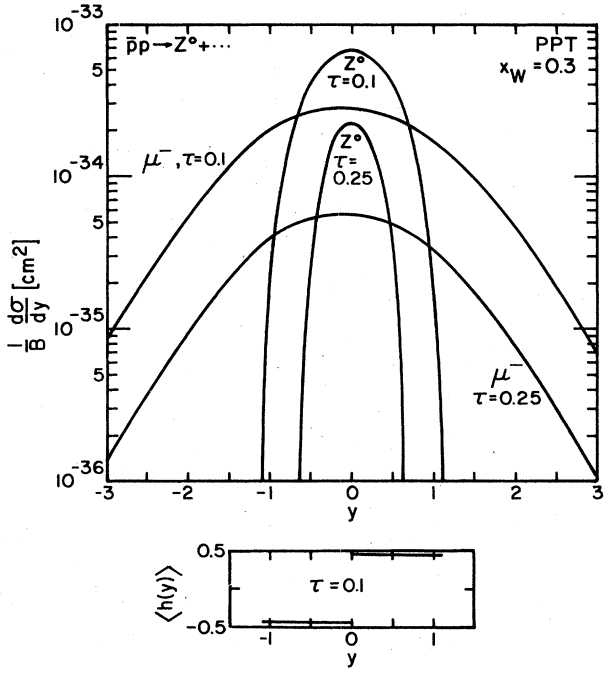

FIG. 44. Angular distributions for $\bar{p}p \to Z^0 + \cdots$ at $\tau = 0.1$ and 0.25, in terms of c.m. rapidity y, and for the decay μ^-, for $\sin^2\theta_W = 0.3$. Distributions for μ^+ are obtained by the replacement $y \leftrightarrow -y$. Also shown is the net helicity of the produced Z^0.

$|y|$. Because the $Zq\bar{q}$ couplings have $V \pm A$ components, the Z is produced less fully aligned than the $W^\pm$ under similar conditions. The influence of the polarization on the angular distributions of the decay products (e.g., μ^+ and μ^-) is quite minor: the mean c.m. energy of the μ^- is expected slightly to exceed that of the μ^+.[22] As was the case for the production and decay of W^+ and W^-, the angular distribution of the decay products is quite broad. The shape of $d\sigma_{\mu^+}/dy$ adequately represents the shape expected for the angular distribution of hadron jets. The largely kinematical two-particle correlations are similar to those discussed in Sec. IV.

The differential cross sections computed for $\bar{p}p$ collisions under the same assumptions are shown in Fig. 44. The predicted alignment of the Z^0 is more intense than in the pp case, but the tiny asymmetry of the μ^- differential cross sections indicates that it is of little practical importance.

Analogous computations based on Field's parton parametrization appear in Figs. 45 and 46.

Problems associated with the detection of the hadronic decays of Z^0 were treated briefly in Sec. IV. What of the leptonic decays? The source of background which is potentially most troublesome probably is the Drell–Yan dilepton production discussed in Sec. III. However, for an intermediate boson of mass $M_Z = 81$ GeV/c^2 with a 5% branching ratio into muon pairs and total width of approximately 2 GeV, as given by the Weinberg–Salam model, the computed signal is more than three orders of magnitude larger than the background under the peak in effective mass. If leptons can be identified reliably, the signal for Z^0 production and decay would seem exceptionally clean.

VI. OUTLOOK

If the mass of the intermediate vector boson does not exceed 100 GeV/c^2, the estimated production cross sections appear adequate to make possible its discovery with the next generation of proton–(anti)proton colliding beam machines. The most desirable machine for this purpose will be one with the highest attainable luminosity at the highest achievable energy. Since the mass of the intermediate boson (and therefore the threshold energy for its production) is not known, it may be prudent to regard c.m. energy as slightly more precious than luminosity, if compromises must be struck.

It is clearly desirable to increase the reliability of cross-section estimates for $W^\pm$ and Z^0 production, or at least to arrive at a better assessment of their reliability. Several categories of experimental information will

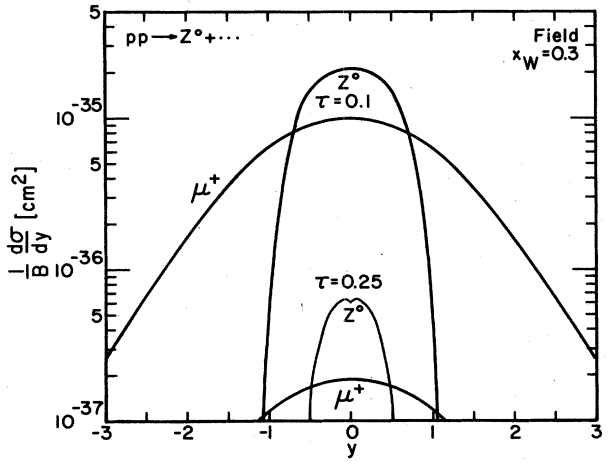

FIG. 45. Same as Fig. 43, for the Field parton distribution.

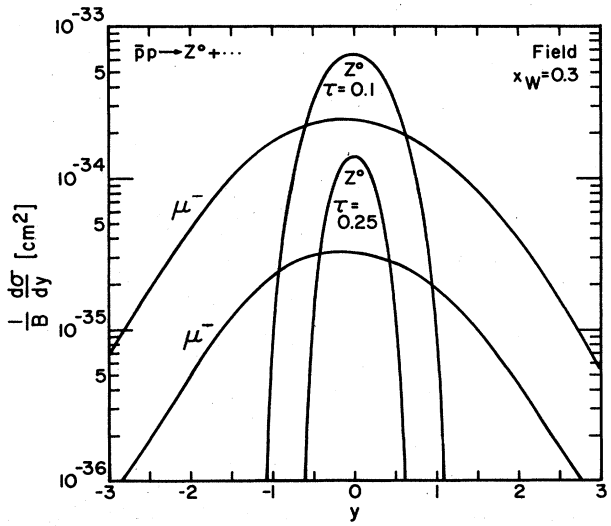

FIG. 46. Same as Fig. 44, for the Field parton distribution.

[22]Similar charge asymmetries have been noted in a related context by Brown, Mikaelian, and Gaillard (1974).

make this possible. The most important series of measurements will be a test of Drell–Yan scaling prediction at dilepton masses far above the resonance region. Corollary studies of the relative rates for massive dilepton production in pp, πp, and $\bar{p}p$ collisions are also of obvious importance. Closely related information on parton distributions within hadrons and on possible deviations from Bjorken scaling, obtained from deep-inelastic lepton scattering experiments, can play a useful supporting role. Progress toward a better-defined theory of the weak interactions, whether in the realm of neutral current phenomenology or in the nature of sharper estimates for M_W and M_Z, will contribute to a more precise answer to the question, "What are we searching for?" Finally, the study of large transverse momentum phenomena in πp and $\bar{p}p$ collisions compared to observations of pp collisions is important for the anticipation of backgrounds.

Is the discovery of the intermediate boson a surer bet in $\bar{p}p$ collisions than in pp collisions? Our current understanding of the mechanism for W production, embodied in the Drell–Yan picture, hangs on two assumptions:

(i) The intermediate boson is produced by a pointlike interaction of a quark and antiquark.

(ii) Both quarks and antiquarks are present (in sufficient numbers) in the colliding hadrons.

The second assumption is naturally less daring for $\bar{p}p$ than for pp collisions, but the first applies equally to both cases. It is my conclusion that for small values of τ, the uncertainty in the number of antiquarks within a proton is insignificant. Consequently, at equal c.m. energies, unless the time average luminosity for a $\bar{p}p$ device is more than 10% of that for a competing pp facility, I see no advantage to antiprotons for the intermediate boson search.

Whereas production cross sections seem quite adequate for the discovery of $W^{\pm}$ and Z^0, the design of an experimental apparatus raises challenges to one's ingenuity. A detector of large aperture, with good lepton identification and precise hadron calorimetry, seems called for. On the basis of the calculations presented in Sec. IV and V it is my judgment that the leptonic decays $W \to l\nu$ and $Z^0 \to l^+l^-$ offer the cleanest signatures. However, the branching ratios for these decays may be quite small, so they must be identified with high efficiency. The time is ripe for serious consideration of the relative merits of leptonic and hadronic decays and of various detection schemes. Among the important issues to be confronted is whether symmetric or asymmetric colliding beam energies are to be preferred.

What if the intermediate boson is not found? Three reasonable explanations can be foreseen:

(i) The estimates of production cross sections are significantly in error. Concurrent measurements of massive dileptons and the application of CVC arguments will provide an internal check of this hypothesis.

(ii) The mass of the intermediate boson exceeds currently popular estimates. This would at least mildly upset the theoretical picture now evolving.

(iii) The intermediate boson does not exist at all. Although unattractively negative, this conclusion would be of fundamental significance, for our entire understanding of the weak interactions would be undermined.

A final barrier to the easy identification of the intermediate bosons should be noted. My entire discussion has been based on the assumption that the only fundamentally new objects to be discovered in the next energy regime are the $W^{\pm}$ and Z^0. This is an unreasonably conservative view. If recent experience is a reliable guide, we may look forward to a new period of splendid confusion in which the discovery of the intermediate boson is made more challenging by the untold richness of other new phenomena.

ACKNOWLEDGMENTS

My interest in the search for the intermediate boson was aroused by a Colliding Beams Workshop organized by Alvin Tollestrup and by the POPAE study group chaired by Bob Diebold. Insistent questions from them and from a large number of other colleagues provided the motivation to prepare this report. I am especially grateful to J. D. Bjorken and B. W. Lee for discussions and encouragement. In addition, helpful comments on the manuscript were made by John Ellis, Francis Halzen, Maurice Jacob, Jon Rosner, Robert Shrock, and Sam Treiman.

I am pleased to thank Angela Gonzales and Robin Perkins for drafting a large number of figures with speed and good humor, and Trudi Legler for typing the manuscript with aplomb and grace.

APPENDIX: CONSERVED VECTOR CURRENT RELATIONS FOR $W^{\pm}$ PRODUCTION

The conserved vector current hypothesis (CVC) connects the cross sections for lepton pair production and intermediate boson production (Okun', 1966; Yamaguchi, 1966; Lederman and Pope, 1971). The W-production cross section can be written as the sum of separate positive contributions from the vector and axial vector charged currents

$$\sigma_W = [\sigma_W]_V + [\sigma_W]_A , \tag{A1}$$

or as an inequality

$$\sigma_W \geq [\sigma_W]_V . \tag{A2}$$

Averaging W^+ and W^- production in pp and pn collisions, and neglecting the contribution of the strangeness-changing current, one obtains the CVC connection

$$\langle \sigma_W \rangle \equiv \tfrac{1}{4}[\sigma_{W^+}(pp) + \sigma_{W^-}(pp) + \sigma_{W^+}(pn) + \sigma_{W^-}(pn)]$$
$$\geq \frac{3G\cos^2\theta_C}{4\alpha^2\sqrt{2}} M_W^4 \left[\frac{d\sigma}{d\mathfrak{M}^2}(pp) + \frac{d\sigma}{d\mathfrak{M}^2}(np)\right]_{\text{isovector}} , \tag{A3}$$

where $[d\sigma/d\mathfrak{M}^2]_{\text{isovector}}$ is the differential cross section for production of a dilepton of mass $\mathfrak{M}$ by isovector virtual photons. Numerically the relation is

$$\langle \sigma_W \rangle \geq 0.22\ (\text{GeV})^{-2} M_W^4 \langle d\sigma/d\mathfrak{M}^2 \rangle_{\text{isovector}} . \tag{A4}$$

If the lepton pair cross section were known at $\mathfrak{M} = M_W$, Eq. (A4) would provide a lower bound on the charge-averaged cross section for W production. In practice

the isospin content of massive virtual photons is of course unknown. Consequently, in place of a rigorous lower bound we have a bound subject to the assumption that isovector photons are solely responsible for dilepton production. This is, strictly speaking, no bound at all. It may nevertheless set a useful target.

REFERENCES

Abers, E. S., and B. W. Lee, 1973, Phys. Rep. **9C**, 1.
Albright, C. H., C. Quigg, R. E. Shrock, and J. Smith, 1976, Phys. Rev. D **14**, 1780.
Altarelli, G., *et al.*, 1975, Nucl. Phys. B **92**, 413.
Anderson, K. J., *et al.*, 1976, "Production of Continuum Muon Pairs at 225 GeV by Pions and Protons," submitted to the XVIII International Conference on High Energy Physics, Tbilisi.
Augustin, J. E., *et al.*, 1975, Phys. Rev. Lett. **34**, 764.
Berman, S. M., J. D. Bjorken, and J. B. Kogut, 1971, Phys. Rev. D **4**, 3388.
Bhattacharya, R., J. Smith, and A. Soni, 1976, Phys. Rev. D **13**, 2150.
Bjorken, J. D., 1976, SLAC–PUB–1841 (unpublished).
Bjorken, J. D., and C. H. Llewellyn-Smith, 1973, Phys. Rev. D **7**, 887.
Blankenbecler, R., *et al.*, 1975, SLAC–PUB–1531 (unpublished).
Brown, R. W., K. O. Mikaelian, and M. K. Gaillard, 1974, Nucl. Phys. B **75**, 112.
Chu, G., and J. F. Gunion, 1975, Phys. Rev. D **11**, 73.
Cline, D., 1975, "New Particles Produced by Neutrinos," University of Wisconsin Report given at the Irvine Conference.
Cronin, J. W., 1976, "Review of Massive Dilepton Production in Proton-Nucleus Collisions," lecture given at the International School of Subnuclear Physics, Erice.
Darriulat, P., 1976, Rapporteur's Talk at the XVIII International Conference on High Energy Physics, Tbilisi.
De Rujula, A., H. Georgi, S. L. Glashow, and H. R. Quinn, 1974, Rev. Mod. Phys. **46**, 391.
Drell, S. D., and T.-M. Yan, 1970, Phys. Rev. Lett. **25**, 316.
Drell, S. D., and T.-M. Yan, 1971, Ann. Phys. (N.Y.) **66**, 578.
Ellis, J., M. K. Gaillard, and D. V. Nanopoulos, 1976, Nucl. Phys. B **106**, 292.
Farrar, G. R., 1974, Nucl. Phys. B **77**, 429.
Feynman, R. P., 1972, *Photon-Hadron Interactions* (Benjamin, Reading, Mass.), Lecture 31.
Field, R. D., and R. P. Feynman, 1976, Caltech report CALT–68–565 (unpublished).
Finjord, J., 1976, NORDITA Report 76/22 (unpublished).
Finjord, J., and F. Ravndal, 1976, Phys. Lett. B **62**, 438.
Fox, G. C., 1976, Invited talk at the 1976 Meeting of the Division of Particles and Fields of the American Physical Society, Brookhaven National Laboratory.
Frisch, H. J., 1976, Invited talk at the 1976 Meeting of the Division of Particles and Fields of the American Physical Society, Brookhaven National Laboratory.
Glashow, S. L., J. Iliopoulos, and L. Maiani, 1970, Phys. Rev. D **2**, 1285.
Goldhaber, A. S., and J. Smith, 1975, Rep. Prog. Phys. **38**, 731.
Golubkov, Yu. A., A. A. Ivanilov, Yu. P. Nikitin, and G. V. Rozhnov, 1974, Sov. J. Nucl. Phys. **18**, 203.
Halzen, F., 1976, Wisconsin report COO-573 (unpublished).
Hanson, G., *et al.*, 1975, Phys. Rev. Lett. **35**, 1609.
Hom, D. C., *et al.*, 1976a, Phys. Rev. Lett. **36**, 1236.
Hom, D. C., *et al.*, 1976b, Phys. Rev. Lett. **37**, 1374.
Jaffe, R. L., and J. R. Primack, 1973, Nucl. Phys. B **61**, 317.
Kluberg, L., *et al.*, 1976, Phys. Rev. Lett. **37**, 1451.
Lederman, L. M., and B. G. Pope, 1971, Phys. Rev. Lett. **27**, 765.
Lederman, L. M., and B. G. Pope, 1976, "Dilepton Production and Scaling" (unpublished).
Lee, B. W., 1976, Summary Talk given at the Aachen Neutrino Conference, Fermilab–Conf–76/61–THY.
Lee, T. D., and C. S. Wu, 1965, Annu. Rev. Nucl. Sci. **15**, 381.
Minh Duong-Van, 1976, Phys. Lett. B **60**, 287.
Mo, L., 1975, in *Proceedings of the 1975 International Symposium on Lepton and Photon Interactions at High Energies*, edited by W. T. Kirk (SLAC, Stanford), p. 651.
Mockett, P., *et al.*, 1975, Fermilab Proposal P–332.
Okada, J., S. Pakvasa, and S. F. Tuan, 1976, Nuovo Cimento Lett. **16**, 555.
Okun', L. B., 1966, Yad. Fiz. **3**, 590.
Okun', L. B., and M. B. Voloshin, 1976, ITEP Preprint No. 111.
Pakvasa, S., D. Parashar, and S. F. Tuan, 1974, Phys. Rev. D **10**, 2124.
Palmer, R. B., E. A. Paschos, N. P. Samios, and L.-L. Wang, 1976, Phys. Rev. D **14**, 118.
Paschos, E. A., and L.-L. Wang, 1976, Comments Nucl. Part. Phys. **6**, 115.
Peierls, R. F., T. L. Trueman, and L.-L. Wang, 1977, Brookhaven preprint (unpublished).
Perkins, D. H., 1975, in *Proceedings of the 1975 International Symposium on Lepton and Photon Interactions at High Energies*, edited by W. T. Kirk (SLAC, Stanford), p. 571.
Perl, M. L., 1975, SLAC–PUB–1592.
Perl, M. L., and P. Rapidis, 1974, SLAC–PUB–1496.
Perl, M. L., *et al.*, 1975, Phys. Rev. Lett. **35**, 1489.
Perl, M. L., *et al.*, 1976, Phys. Lett. B**63**, 466.
Rubbia, C., P. McIntyre, and D. Cline, 1976, Harvard preprint (unpublished).
Salam, A., 1968, in *Elementary Particle Theory: Relativistic Groups and Analyticity (Nobel Symposium No. 8)*, edited by N. Svartholm (Almqvist and Wiksell, Stockholm), p. 367.
Sciulli, F., 1975, in *Particles and Fields-1975*, edited by H. J. Lubatti and P. M. Mockett (University of Washington, Seattle), p. 76.
Sivers, D., S. J. Brodsky, and R. Blankenbecler, 1976, Phys. Rep. C **23**, 1.
Sullivan, J. D., 1976, in *Particle Searches and Discoveries-1976*, edited by R. S. Panvini (AIP, New York), p. 142.
Taylor, J. C., 1976, *Gauge Theories of Weak Interactions* (Cambridge U.P., London).
Taylor, R. E., 1975, in *Proceedings of the 1975 International Symposium on Lepton and Photon Interactions at High Energies*, edited by W. T. Kirk (SLAC, Stanford), p. 679.
Tsai, Y.-S., 1971, Phys. Rev. D **4**, 2821.
Weinberg, S., 1967, Phys. Rev. Lett. **19**, 1264.
Weinberg, S., 1971, Phys. Rev. Lett. **27**, 1688.
Yamaguchi, Y., 1966, Nuovo Cimento **43**, 193.